



Repositorio Institucional de la Universidad Autónoma de Madrid

<https://repositorio.uam.es>

Esta es la **versión de autor** del artículo publicado en:

This is an **author produced version** of a paper published in:

Biochimica et biophysica acta. Molecular basis of disease 1842.7 (2014):
1059-1070

DOI: <http://dx.doi.org/10.1016/j.bbadis.2014.03.013>

Copyright: © 2014 Elsevier B.V. All rights reserved

El acceso a la versión del editor puede requerir la suscripción del recurso
Access to the published version may require subscription

**BULK AUTOPHAGY, BUT NOT MITOPHAGY, IS INCREASED IN CELLULAR
MODEL OF MITOCHONDRIAL DISEASE.**

María Morán^{1,2*}, Aitor Delmiro ^{1,2}, Alberto Blazquez^{1,2} , Cristina Ugalde^{1,2}, Joaquín Arenas ¹,
Miguel A. Martín ^{1,2}.

¹Mitochondrial and Neuromuscular Diseases Laboratory, Hospital Universitario 12 de Octubre
Research Institute (i+12), Madrid, Spain; ² Spanish Network for Biomedical Research in Rare
Diseases (CIBERER), U723, Spain.

*Corresponding author: Dr. María Morán, Laboratorio de enfermedades raras: mitocondriales
y neuromusculares. Instituto de Investigación Hospital Universitario 12 de Octubre (i+12).
Centro de Actividades Ambulatorias, 6ª planta. Avenida de Córdoba s/n, 28041 Madrid. Phone:
+34 91 779 2784, FAX: +34 91 390 8544, e-mail: mmoran@h12o.es

Authors declare no conflict of interest

Abstract

Oxidative phosphorylation system (OXPHOS) deficiencies are rare diseases but constitute the most frequent inborn errors of metabolism. We analyzed the autophagy route in 11 skin fibroblast cultures derived from patients with well characterized and distinct OXPHOS defects. Mitochondrial membrane potential determination revealed a tendency to decrease in 5 patients' cells but reached statistical significance only in 2 of them. The remaining cells showed either no change or a slight increase in this parameter. Colocalization analysis of mitochondria and autophagosomes failed to show evidence of increased selective elimination of mitochondria but revealed more intense autophagosome staining in patients' fibroblasts compared with controls. Despite the absence of increased mitophagy, Parkin recruitment to mitochondria was detected in both control and patients' cells and was slightly higher in cells harboring complex I defects. Western blot analysis of the autophagosome marker LC3B, confirmed significantly higher levels of the protein bound to autophagosomes, LC3B-II, in patients' cells, suggesting an increased bulk autophagy in OXPHOS defective fibroblasts. Inhibition of lysosomal proteases caused significant accumulation of LC3B-II in control cells, whereas in patients' cells this phenomenon was less pronounced. Electron microscopy studies showed higher content of late autophagic vacuoles and lysosomes in OXPHOS defective cells, accompanied by higher levels of the lysosomal marker LAMP-1. Our findings suggest that in OXPHOS deficient fibroblasts autophagic flux could be partially hampered leading to accumulation of autophagic vacuoles and lysosomes.

Keywords: autophagy, OXPHOS deficiency, Parkin, autophagosome, mitophagy, lysosome.

1. INTRODUCTION

Autophagy is a route of degradation of cellular components that can be induced by different stimuli. Several forms of autophagy exist and among them, macroautophagy (hereafter autophagy), involves the formation of double-membrane vesicles called autophagosomes that enwrap and sequester the cellular component to be eliminated (for a review see [1]). After cargo sequestration, autophagosomes fuse with lysosomes that will digest the sequestered material, allowing recycling of some of its components or supporting energy production. This type of autophagy is, so far, the only known route to clear large structures and entire organelles, such as mitochondria. Although this pathway was mainly considered as a bulk sequestration process, selective autophagy to degrade excessive or damaged organelles was initially described by Kissova et al [2], and to emphasize the non-random elimination of defective mitochondria, the term mitophagy was proposed [3]. In recent years mitophagy has been related to dissipation of mitochondrial membrane potential ($\Delta\Psi$), which could trigger the elimination of the organelle [2, 4-8]. Since the beginning of this century it has been highlighted that mitochondria are dynamic organelles that continuously fuse and divide. These processes, generally termed mitochondrial dynamics, fine-tune fundamental cellular pathways, and alterations in them can constitute both cause and effect of disease [9]. It has been proposed that after fission, if the resulting mitochondria are dysfunctional and not able to repolarize, fusion is impaired and mitochondria are kept in an isolated state in which they are tagged and recruited for digestion and elimination by autophagy [2, 4-8, 10, 11]. Thus, autophagy and mitochondrial dynamics would cooperate to target dysfunctional mitochondria for elimination and would help maintaining the bio-energetic efficiency of the cell. Nevertheless, the selective inhibition of mitochondrial fusion by mitochondrial dysfunction has been only demonstrated in yeast [12], and how mitochondrial dynamics could aid in the elimination of dysfunctional mitochondria is still a matter of research.

Primary mitochondrial diseases (MD) caused by dysfunction of the oxidative phosphorylation system (OXPHOS) are the most frequent inborn errors of metabolism. Cells from MD patients show decreased $\Delta\Psi$ due to diminished electron flow through the respiratory chain [13-18], suggesting that the selective elimination of defective mitochondria in cells from patients with MD could be increased. Nevertheless, this possibility has not been studied in depth. In fact, only three reports exist describing increased mitophagy in cells from patients with primary coenzyme Q deficiency and patients with coenzyme Q deficiency associated with mutations in mitochondrial DNA (mtDNA) [19-21]. In tissues from animal models of MD evidence of increased autophagy has been reported. For instance, in a mouse model of mitochondrial myopathy due to mutation in the mitochondrial helicase Twinkle, evidence of an increased autophagic starvation-like response, involving mitophagy in skeletal muscle, has been described [22, 23]. In addition, in a murine model of dominant optic atrophy, an increased amount of autophagosomes was found in retinal ganglion cells [24]. These evidences support the hypothesis that mitochondrial deficiency could induce a stress signal leading to increased autophagy as compensatory response, either to obtain energy or to eliminate damaged mitochondria that could induce further cellular dysfunction.

The goal of our study was to evaluate the autophagic response in primary skin fibroblasts derived from 11 MD patients, with well characterized and distinct mutations in nuclear and mitochondrial OXPHOS genes, and to further analyze the role of mitophagy in the pathophysiology of MD. These cells were divided in 4 differentiated groups attending to the respiratory chain deficiency they presented: (i) fibroblasts with isolated complex I deficiency due to mutations in *NDUFV1* and *NDUFA1* (n=3); (ii) fibroblasts with complex III deficiency harboring mutations in the complex III assembly factor *BCS1L* (n=5); (iii) fibroblasts with mutations in the complex IV assembly factor *SURF1* and in the mitochondrial encoded complex IV gene *COX2* (n=2); and (iv) one cell line with decreased mitochondrial content due to mutations in *SUCLG1*.

2. MATERIALS AND METHODS

2.1 Cell culture and treatments

Skin fibroblasts from MD patients were cultured in DMEM with high glucose (4.5 g/L) supplemented with 10% fetal calf serum, penicillin 50 IU/mL and streptomycin 50 IU/mL. Cells were routinely checked to be free of mycoplasmas.

Respiratory chain (RC) deficiency detected in each cell line and the patients' (P) main genetic data are shown in **Table 1**. Cell lines from P1-P3 showed isolated complex I deficiency due to mutations in either the complex I catalytic subunit NDUFV1 or in the structural subunit NDUFV1 [25, 26]. Cell lines from P4-P6 and P8 showed either isolated or combined complex III deficiency due to mutations in the complex III assembly factor BCS1L[27-30], whereas P7 did not show significant alteration of RC activities in fibroblasts but decreased complex III in skeletal muscle [30]. P9 and P10 showed complex IV deficiency due to mutations in the assembly factor SURF1 and in the structural subunit COX2 respectively, the latter showing 60% heteroplasmy [31]. The combined RC deficiency found in P11 was due to decreased levels of mitochondrial DNA caused by mutations in *SUCLG1* [32].

We have studied fibroblasts from skin biopsies obtained for research purposes after written informed consent. The research was approved by the Ethics Committee at *Hospital 12 de Octubre* and is in accordance with the Helsinki Declaration.

To analyze autophagy-dependent degradation of LC3, cells were maintained in culture medium with freshly prepared E64d and pepstatin A (Sigma) at 10 µg/mL in DMSO for 4 h according to Kimura et al [33]. Cells were washed with ice-cold PBS, scraped and centrifuged at 800 x g for 5 min at 4° C. Cells were subsequently resuspended in lysis buffer and western blot analysis was performed to detect LC3B as described below.

2.2 Western blot analysis in cell lysates

Fibroblasts were lysated in 5 mM Tris pH 8.0, 20 mM EDTA, 0.5 % Triton X-100, protease and phosphatase inhibitor cocktail (Roche), centrifuged at 11.000 x g, and supernatant was collected. Protein content of the supernatants (cell lysates) was determined [34] . Samples of cell lysates (5-10 µg) were used to perform semi-quantitative analysis, by Western Blot, of the levels of: LC3B (anti-LC3B Sigma), LAMP-1 (anti-LAMP-1 G1/139/5, DHSB), and pyruvate dehydrogenase E1 alpha (PDH-E1-α), complex II 70 kDa subunit (SDHA), and Complex V α subunit (CVα), all from Mitosciences. Immunodetection of primary antibodies was carried out with peroxidase-conjugated secondary antibodies (GE Healthcare). The signal was detected with Enzyme Chemiluminescence (Novex® ECL HRP Chemiluminiscent Substrate Reagent Kit, Life Technologies S.A.). Band densities were evaluated by densitometric scanning (Image J software). β actin or α tubulin were immunodetected with mouse anti-β actin and anti-α tubulin (both from Sigma) and used as loading control.

2.3 ATP content measurements

Cellular ATP was extracted from cells in boiling 100 mM Tris, 4 mM EDTA pH 7.75, and assayed by bioluminescence using a luciferin-luciferase system (Roche) according to manufacturer's instructions. ATP concentration was corrected by cell number and expressed as percentage of control cells' ATP content.

2.4 Confocal microscopy in living cells

Mitochondrial membrane potential ($\Delta\psi$) was analyzed by confocal microscopy in living cells as described by Davidson et al[35]. In brief, plasma membrane was depolarized by the addition of

potassium to 50 mM and cells were loaded with 30 nM tetramethylrhodamine methyl ester (TMRM) for 60 min in a CO₂ incubator. Image collection was carried out in cells maintained at 37° C with a 40x lens using 543 nm laser set at 1.5% intensity. TMRM intensity per cell was analyzed with Image J software and corrected by citrate synthase activity, a classical marker of cellular mitochondrial content that was determined in cultured cells as described elsewhere [36].

To evaluate lysosomal content living fibroblasts were loaded with 50nM LysoTracker™ DND-26 (Molecular Probes) for 90 min in the dark in a CO₂ incubator. Image collection was carried out with a 40x lens using the 488 nm excitation laser line set at 2% intensity, with cells maintained at 37° C. Cells were imaged randomly with 1 µm slices and 1024x1024 pixel resolution. LysoTracker intensity per cell was analyzed with the Image J software. No enhancement of the original images was done.

2.5 Immunofluorescence

Immunofluorescence was performed on sub-confluent paraformaldehyde-fixed cells. Mouse monoclonal anti-C Vα (MitoSciences), and rabbit anti-LC3B or anti-Parkin (Sigma) were used as primary antibodies. Texas Red-conjugated anti-mouse (MitoSciences) and Alexa-488-conjugated anti rabbit were used as secondary antibodies. Coverslips were mounted in ProLong Gold© antifade reagent (Molecular Probes) on glass slides. Cells were viewed with a Zeiss LSM 510 Meta confocal microscope with a 63x planapochromat oil immersion objective (NA: 1.42), sequential scanning of green and red channels were performed to avoid bleed-through effect. Cells were imaged randomly with 0.5-0.7 µm slices and 1024x1024 pixel resolution. For colocalization analysis we used the plugin “Colocalization” and the plugin “JaCOP” to determine Manders’ coefficients, both from Image J. No enhancement of the original images was done.

2.6 Electron microscopy (EM)

Adherent non confluent cells were fixed in 2% glutaraldehyde and 4% paraformaldehyde in 0.1 M sodium phosphate buffer (pH 7.4) for 90 min at room temperature, washed with PBS and then post-fixed in 1% OsO₄ for 1 h at 4° C. After dehydration in graded series of ethanol, the cells were embedded in Epon 812 (Fluka) and polymerized at 60° C for 2 days. Ultrathin sections (90 nm) were analyzed in a JEOL JEM1010 transmission electron microscope equipped with a 4Kx4K TemCam-F416 digital camera (TVIPS, Gauting, Germany). Identification of autophagosomes, late autophagic vesicles, lysosomes and estereological counting was performed as described previously [37-40].

2.7 Data Analysis

All experiments, except electron microscopy, were performed at least in triplicate. Data are presented as mean ± standard deviation (SD). Six different control primary skin fibroblasts were used in the present study, and 4 to 6 different controls were evaluated for the determination of each parameter. Due to the poor growth rate of patients' cells not all the determinations could be performed in all patients' cell lines. Statistical analysis was performed with the SPSS software (SPSS, Chicago, IL) and statistical significance was set at $P < 0.05$. When Kruskal-Wallis test was applied, to minimize the risk of statistical error type 1, after *post hoc* analysis we only performed comparison between control and patients' groups. Densitometry of western blots and confocal images analysis were performed with Image J (Rasband, W.S., ImageJ, U. S. National Institutes of Health, Bethesda, Maryland, USA, <http://imagej.nih.gov/ij/>, 1997-2012). To perform the analysis of lysosomal flux, LC3B-II/actin ratio in non-treated cells were set as basal values of the autophagic marker for each cell line, and increases in LC3B-II/actin in protease inhibitors-treated cells were expressed as a percentage of its basal values.

3. RESULTS

3.1 Mitochondrial dysfunction causes mild alterations in mitochondrial membrane potential and decreased ATP content

To assess if $\Delta\psi$ is lower in the MD cells and mitophagy could be induced, we determined this parameter by confocal microscopy as mean TMRM fluorescence per cell in eleven MD primary skin fibroblasts showing: complex I deficiency due to mutations in *NDUFV1* and *NDUFA1* (P1-P3), complex III deficiency caused by mutations in the assembly factor of this complex, *BCS1L* (P4-P8), two cell types with mutations in the complex IV assembly factor *SURF1* and the mitochondrial encoded complex IV gene *COX2* (P9, P10), and one cell culture with decreased mitochondrial content due to mutations in *SUCLG1* (P11) (Figure 1A). Statistical analysis demonstrated a significant cell line effect (Kruskal Wallis test $P = 0.047$). Mean $\Delta\psi$ was decreased in P1, P3 and P8-P11, and *post-hoc* analysis revealed significantly lower levels in P9 and P10, both affected by complex IV deficiencies. On the contrary, a slight hyperpolarization was detected in P4 and P5, both affected by a complex III enzymatic defect.

We have previously shown that in the CI-deficient cells analyzed in the present investigation ATP content is significantly lower compared to control cells [26]. To assess the bionergetic state in the remaining MD cells we also determined the ATP content, finding, in agreement, significantly lower levels of this parameter in complex III-deficient cells and P11 (Figure 1B, Mann-Whitney test $P = 0.01$ for patients vs. controls).

3.2 Mitochondrial dysfunction induces increased autophagic response but does not alter mitophagy

Mitophagy was assessed in MD cell lines, by confocal microscopy analysis of mitochondria labeled with an antibody against complex V α subunit (CV α) , and autophagosomes labeled

with an antibody against the classical marker of these structures, LC3B [41]. The autophagosome staining pattern revealed a more intense signal in MD cells in comparison with control cells, regardless of their mean mitochondrial membrane potential, displaying LC3 *puncta* and also patched signal (Figure 2). Nevertheless, colocalizations between fragmented mitochondria and autophagosomes were very scarce, even in cells with high amounts of fragmented mitochondria, *i.e.* from P8. Only in few cases small dotted mitochondria colocalized with LC3 *puncta*, and most of the colocalization detected occurred in reticular mitochondria suggesting that only a small number of fragmented mitochondria were being selectively eliminated (see Figure 2, P6 inset). Colocalization according to Mander's coefficients, was low in both controls and MD cells, although a slight increase in Mander's coefficient for the green channel in the patients' fibroblasts was detected (Mander's coefficients for the red channel were 0.128 ± 0.09 for controls' cells and 0.093 ± 0.08 for MD cells, and Mander's coefficients for the green channel were 0.154 ± 0.08 for controls' cells and 0.234 ± 0.13 for MD cells). Images of control and MD fibroblasts with both channels separately depicted are shown in Supplemental Figures 1A and 1B, also the quantitative analysis of mean LC3B fluorescence *per cell* is shown in Supplemental Figure 1C (Mann-Whitney test $P = 0,014$ for patients *vs.* controls). These findings would indicate that bulk autophagy is higher than normal in MD fibroblasts, but this phenomenon is not due to augmented elimination of defective mitochondria.

As CV α was used as a mitochondrial marker in our immunofluorescence assays, we tested the levels of this protein in the MD cells to exclude putative alterations in the mitochondrial network staining that could bias our findings. Western blot analysis showed that CV α levels were not decreased by the OXPHOS deficiencies present in our MD cells (Figure 3A). If increased mitophagy occurred due to OXPHOS deficiency, we could expect lower mitochondrial content in the MD cells compared with those of healthy controls. Previous data from our laboratory have shown that the levels of several key mitochondrial proteins (SDHA,

CORE2, COX2) were not generally lower than normal in fibroblasts P2-P8, suggesting that their mitochondrial content was neither affected [25, 26, 30]. To further corroborate that mitochondrial content was not altered in any of the MD cells studied in the present work we analyzed the levels of key mitochondrial proteins, such as complex II 70 kDa subunit (SDHA) and the mitochondrial matrix protein pyruvate dehydrogenase E1-alpha (PDH-E1- α) because these proteins are commonly used as mitochondrial content markers. The levels of these proteins were not significantly lower in the MD cells compared with the controls (Figure 3B). Analysis of the densitometry of CV α , SDHA and PDH-E1- α are shown in Supplemental Figure 2. Levels of SDHA, CV α and PDH-E1- α in 6 different control fibroblasts and 2 MD cells (P1 and P4) are shown in Figure 3C. These findings suggest that the mitochondrial content is not altered in any of MD cells analyzed, in agreement with previous research from our group [26].

We also checked the levels of protein markers for other organelles (peroxisomes, endoplasmic reticulum and Golgi apparatus), but overall we did not detect lower values in the MD cells studied (Supplemental Figure 3). These results indicate that increased autophagy in the MD fibroblasts do not seem to induce the specific elimination of any organelle, *i.e.*, mitochondria, peroxisomes, endoplasmic reticulum, or Golgi apparatus.

To analyze if the absence of mitophagy in MD-derived fibroblasts could be due to defective recruitment of dysfunctional mitochondria to autophagy, we studied the molecular labeling of mitochondria with Parkin (Figure 4). The analysis of double-stained cells with anti-Parkin and anti-CV α antibodies showed punctated Parkin signal. Colocalization between Parkin and mitochondria was evident, in fragmented and isolated mitochondria, and also in mitochondria of tubular shape in both control and MD fibroblasts. Images of control and MD fibroblasts with both channels separately depicted are shown in Supplemental Figure 4A and 4B. Interestingly, fibroblasts affected by complex I deficiency (P1-P3) showed more intense Parkin staining in tubular mitochondrial network than control cells. Mander's coefficient for the red

channel were 0.537 ± 0.2 (control fibroblasts), 0.642 ± 0.014 (P1), 0.768 ± 0.06 (P2) and 0.880 ± 0.01 (P3). Mander's coefficient for the green channel were 0.280 ± 0.07 (control fibroblasts); 0.272 ± 0.05 (P1); 0.233 ± 0.06 (P2) and 0.151 ± 0.02 (P3).

Although we could not find increased mitophagy in patients' fibroblasts, increased LC3B staining in MD cells was shown by immunofluorescence. Therefore, we determined the basal levels of autophagy by western blot analysis of LC3B in total cell lysates. Higher levels of LC3B-II, the LC3 form associated with autophagosomes, was found in the patients' cell lines (Mann-Whitney test $P = 0.013$ for patients vs. controls) (Figure 5A and Figure 5B). These results indicate higher autophagosome content in the cells from MD patients. Normal range of LC3B in six different control cell lines is shown in Figure 5C with two MD cells (P1 and P4) for better comparison between patients and controls.

3.3 Autophagosome clearance is not altered in the autophagic response in mitochondrial diseases but autophagic vacuoles are accumulated in fibroblasts derived from MD patients

To analyze if the increased LC3B-II detected in the patients' cells lysates was due to a failure of lysosomal activity we treated the cells with protease inhibitors E64D and pepstatin A (Figure 6). Control fibroblasts treated with the protease inhibitors showed higher (+150%) amounts of LC3B-II in comparison with vehicle-treated cells, as expected for normal lysosomal-dependent autophagosome clearance. In most of the MD cell lines we could detect milder increases in the mean LC3B-II/actin ratio, but P1, P2 and P11 showed increases in mean LC3B-II/actin ratio similar to those found in controls. Patients cell lines pooled showed 138 % higher levels compared with controls. The statistical analysis of the autophagosome clearance did not show statistical significance between the behavior of MD and control cell lines (Mann-Whitney test $P = 0.315$ for patients vs. controls).

We also studied the colocalization between LC3B and mitochondria by immunofluorescence in bafilomycin A1-treated cells to analyze if under conditions of blocked lysosomal flux we could detect higher levels of mitophagy in MD cells compared with controls. After bafilomycin treatment we did not detect any change in the colocalization between mitochondria and autophagosomes in controls (Mander's coefficients are shown in Supplemental Table 1, and representative images of control and P1-treated cells are shown in Supplemental Figure 5). In MD cells after bafilomycin A1 treatment Mander's coefficient for the red channel was slightly higher but remained very low and was similar to that in bafilomycin-treated controls. These results indicate that there is low colocalization between mitochondria and autophagosomes, and rules out the possibility that increased mitophagy in basal conditions in MD cells could be masked by lysosomal degradation of mitochondria-containing autophagosomes.

Transmission electron microscopy revealed that the most outstanding feature of MD cells in the cryosections was a higher amount of cytosolic vacuoles (Figure 7A), but we could not find evidences of alterations in the mitochondrial ultrastructure of MD cells (Supplemental Figure 6A). Some of these vacuoles could be considered autophagosomes, and hardly any contained mitochondria. The most abundant vesicles were multilaminar bodies, vacuoles containing electrondense material and vacuoles with a mixed appearance between both multilaminar bodies and electrondense vacuoles (examples of these organelles are shown in Supplemental Figure 6B). These organelles covered extensive areas in patients' cells and were often large. According to the morphology criteria of Eskelinen these vacuoles were considered lysosomes, late or degradative autophagic vacuoles (AVd) and vacuoles due to the fusion between AVd and lysosomes, respectively [38-40]. The stereological counting of AVd and AVd fused with lysosomes revealed increased amounts of these organelles per μm^2 in the patients' cells in comparison with control fibroblasts (Figure 7B) (Mann-Whitney test $P < 0.01$ for patients vs. controls).

To confirm that the higher amount of AVd in the patients' cells was accompanied by higher amounts of lysosomes, we performed a western blot against the lysosomal marker LAMP-1 (Figure 8A). The results obtained showed markedly higher levels of this glycoprotein in all patients' cells in comparison to controls (Mann-Whitney test $P=0.016$ for patients vs. controls (Figure 8B). Normal range of LAMP-1 levels in 6 different controls are shown in Figure 8C with 2 MD cells (P1 and P4) for better comparison between patients and controls.

In addition, specific lysosome staining with LysoTracker™ DND-26 in living cells, showed by confocal microscopy higher lysosomal content in MD fibroblasts (Figure 9) (Mann-Whitney test $P=0.007$ patients vs. controls). These results support that higher than normal amounts of lysosomes are present in MD patients' derived fibroblasts.

mTORC1 activity is not decreased in fibroblasts derived from MD patients

To further analyze the state of the autophagic pathway in MD cells, we determined the phosphorylation levels of P70S6 kinase at threonine 389, which is a direct target of mTORC1, a protein complex that negatively regulates autophagy. The results obtained are shown in Supplemental Figure 7. The ratio of phosphorylated p70 S6 kinase/total p70 S6 kinase tended to be higher in most patients' cells in comparison with controls, but the analysis did not reach statistical significance (Mann-Whitney test $P > 0.05$ for patients vs. controls). These results suggest that there is no inhibition of mTORC1 in patients' fibroblasts.

4. DISCUSSION

We have shown that mitophagy is not increased in fibroblasts harboring defects in the OXPHOS system but autophagosomes, lysosomes and late autophagic vacuoles are accumulated. This phenomenon could be caused either by an induction of non-selective autophagy due to a pseudo-starvation response, or to an alteration of the autophagic degradation pathway due to disturbances in some steps of the lysosomal degradation route leading to the accumulation of partially degraded cellular materials.

Abolished mitochondrial membrane potential due to protonophore treatment causes the recruitment of Parkin to mitochondria to mediate their elimination by the autophagic machinery in order to maintain bio-energetic efficiency in the cell [42]. Decreases in mitochondrial membrane potential have been previously reported in cells from patients with OXPHOS disorders suggesting that increased mitophagy could also occur in MD models [14-18]. In our work only 2 cell lines showed lower than normal $\Delta\psi$, and similar results were described previously by Iuso et al., who found, either no alterations or lower $\Delta\psi$, in fibroblasts from complex I-deficient patients [13]. Perhaps the fact that the decreases in $\Delta\psi$ in our MD cells were milder than full depolarization could be the cause of the absence of mitophagy. However, we have previously demonstrated in P1 and P3 that after mitochondrial depolarization and fragmentation, mitochondrial network fusion, a phenomenon dependent on $\Delta\psi$ recovery, was delayed in comparison with control cells, indicating that OXPHOS deficiencies cause slower kinetics of $\Delta\psi$ recovery [26]. Therefore, determination of $\Delta\psi$ in steady-state conditions cannot always reveal dynamic alterations of $\Delta\psi$ occurring in MD cells that could lead to increased mitophagy. Despite the heterogeneity of the MD cell lines analyzed in the present work (i.e., with differences in $\Delta\psi$ alteration, in the severity of the respiratory defect, isolated deficiencies in some patients vs. combined defects in others, or mutations in nuclear DNA vs. mutations in mtDNA), we detected overall higher than normal

levels of the autophagosomal marker LCB-II in all MD cells, suggesting increased autophagy, as previously reported in other models of MD (17-22). Therefore, enhancement of autophagosome content but not increased mitophagy might be a general cellular response to OXPHOS defect that occurs independently of $\Delta\Psi$ and of the severity of the OXPHOS defect.

Previous studies in primary cultures of fibroblasts derived from patients with OXPHOS disorders have described increased mitophagy [19-21]. The discrepancies between these studies and the present findings could be due to the different consequences at cellular level of the OXPHOS disorder shown between the cells studied. For instance, in the studies by Sanchez-Alcazar's group all MD cells showed coenzyme Q deficiency, combined respiratory chain deficiency, decreased $\Delta\Psi$, mitochondrial fragmentation, increased levels of oxidative stress eventually leading to opening the mitochondrial transition pore, and evidences of autophagy induction, such as increased Atg5 and Beclin levels[19-21]. In the present investigation none of the analyzed MD cells showed concurrently those alterations, *i.e.* none presented with decreased $\Delta\Psi$, increased ROS levels and mitochondrial fragmentation at the same time [26] [30]. Moreover, in the MD cells analyzed in the present work we failed to detect changes in Atg5-Atg12, and preliminary data from our laboratory suggest the absence of increased phosphorylation of ULK1 at Ser555 (data not shown), indicating that the initial steps of the autophagic cascade are not induced. It is tempting to speculate that several signals of mitochondrial damage, as strong depolarization and increased mitochondrial ROS production are needed to induce mitophagy. In this regard, it has been reported that both, loss of mitochondrial $\Delta\Psi$ and mTORC1 inhibition, are needed synergistically to induce mitophagy in cells carrying pathogenic mtDNA mutations [43]. Accordingly, yeast cells treated with the complex III inhibitor antimycin A, at concentrations to induce mild mitochondrial alterations, showed increased autophagy but no mitophagy [44]. Further studies are needed to unveil the different autophagic response found in OXPHOS-deficient cells and the trigger(s) responsible for such phenomenon. On the other hand, it has been shown that cells can spare their

mitochondria from degradation even after autophagy induction [45-47]. Mitochondria are key organelles for cell survival; therefore, despite their OXPHOS defects, cells may keep mitochondria out of degradation, preventing a futile cycle of biogenesis and elimination of these vital organelles in a cellular context of lack of energy.

In contrast to previous studies indicating that Parkin labels depolarized mitochondria to initiate mitophagy, we have shown the absence of Parkin-driven mitophagy even in those cell lines with diminished $\Delta\Psi$. These discrepancies could be due to differences in the models of study employed, *i.e.*, strong mitochondrial depolarization with protonophores vs. milder depolarization conditions due to OXPHOS defects, overexpression of Parkin vs. endogenous levels of the protein, or use of cultured cell lines vs. primary cultures [8, 42, 48-50]. Other authors using primary mammalian cell cultures, such as cortical neurons, have also failed to show Parkin-mediated mitophagy, even after CCCP-induced mitochondrial depolarization despite significant Parkin localization to mitochondria [51]. In primary fibroblasts from Parkinson's disease patients harboring PINK1 mutations (a model in which alterations of Parkin behavior are expected) additional external stress stimuli, such as valinomycin treatment, is needed to visualize differences in Parkin levels and its translocation to mitochondria between control and mutant cells [52]. Moreover, it has been reported that in dopaminergic neurons of MitoPark mice, dysfunctional mitochondria do not recruit Parkin *in vivo*, and neither the clearance of dysfunctional mitochondria nor the neurodegenerative phenotype of the animal was affected by absence of Parkin [53]. In the present work we found Parkin labeling not only in small dotted mitochondria (that may be partly depolarized), but also in those expected to have normal mitochondrial potential showing tubular shape, in both controls' and patients' derived cells. These findings are in agreement with previous data showing that, under basal conditions, Parkin exists in the cytoplasm and also directly associated with mitochondria [51, 54-57]. Also, in trans-mitochondrial cybrid cells genetic- and chemically-induced loss of $\Delta\Psi$ triggered Parkin recruitment to mitochondria without causing mitophagy [43]. Given that

mitochondrial Parkin localization was slightly higher in some MD patients' cells without inducing mitophagy, Parkin could be maybe mediating some additional functions different from mitochondrial labeling for autophagy. In fact, several Parkin roles related to mitochondrial function have been reported [55, 56]. For instance, mitochondrial localized Parkin is able to prevent CCCP-induced mitochondrial depolarization in COS-1 and HeLa cells [57]. Interestingly Vincow et al. demonstrated that Parkin mediates selective nonmitophagic turnover of mitochondrial respiratory chain proteins in *Drosophila in vivo* [58], and it has been proposed that some respiratory chain complexes, such as complex I, may be especially labile and would require more frequent turnover than other components [59]. Thus, in complex I-deficient cell lines the increased mitochondrial Parkin recruitment to mitochondria could be maybe related to a role of this protein in mitochondrial membrane potential maintenance under bio-energetic stress conditions, or also in the event of increased respiratory chain component turnover due to altered folding of the mutated subunits, instability or disassembly of respiratory complexes. Findings obtained in autophagy-defective yeast mutants have shown that supply of amino-acids via bulk autophagy, but not selective autophagy, is important for the maintenance of respiratory chain function during starvation [60]. Despite the evolutionary distance between yeast and mammalian cells, these results could suggest that in MD cells, which are under bio-energetic stress conditions and probably under proteinaceous stress due to altered respiratory complexes assembly, autophagy of cytoplasmic material might also be needed to maintain increased turnover of respiratory chain subunits and complexes.

Although autophagy has received more recent attention as a route to clear dysfunctional organelles, it has been known for many years that autophagy is an important survival mechanism during short-term starvation to degrade non-essential components in order to obtain nutrients for vital biosynthetic reactions [37]. Several studies have described starvation-like response in mouse models of MD and human muscle from patients harboring m.8344 A>G mutation [22, 23, 61, 62]. Although MD patients, MD animals or MD cellular models are not

under starvation conditions, their bio-energetic defect prevents them from obtaining high enough ATP levels to maintain normal cellular functions [26, 30]. Low levels of ATP in patients' cells could trigger autophagy due to inhibition of mTORC1 by activation of AMPK, but our preliminary results suggested no inhibition of mTORC1 in the MD cells (supplemental Figure 1). Perhaps, persistent autophagy induction in our model of disease due to chronic low ATP could cause reactivation of mTOR as previously reported by Yu et al in rat kidney cells[63] . New insights in the regulation of the autophagic response in yeast have been recently reported by Graef and Nunnari, who proposed that mitochondrial function can modulate autophagy independently of mTOR through PKA, by affecting both *ATG* gene induction and the autophagic flux (via assembly of Atg into the pre-autophagosomal structures) [64]. The authors proposed that mitochondrial dysfunction blocks both autophagy induction and autophagic flux, and that the response induced may vary depending on the nature and severity of the mitochondrial defect, *i.e.*, collapse of mitochondrial membrane potential vs. only respiratory chain defect. If this regulatory mechanism could also be applied to mammalian cells, we would expect both the inhibition of the autophagic flux and of Atg induction in the MD cells studied in the present work. This would explain the poor response of the MD cells to lysosomal inhibitors, while LC3B-II accumulation would result of partially blocked lysosomal flux. Nevertheless, as the autophagosomal flux was only partially hampered in our MD cells, direct assessment of mTORC1 activity and an in-depth study of the signaling pathways involved in autophagy regulation could help unveil the mechanisms of autophagy regulation in our cellular model of disease.

Decreases in ATP levels can also block the autophagy flux independently of mTORC1 because ATP is required in the sequestration step as well as to maintain lysosomal function [65-69]. Taken into account that mTORC1 seemed to be active but the amount of AVd was significantly increased in our MD cells, we could hypothesize that in fibroblasts harboring OXPHOS defects, autophagic flux could be partially hampered by the lack of energy. This possibility may explain

that after lysosomal inhibition LC3B-II was only slightly increased in patients' fibroblast. Similar results were found in OXPHOS deficient cells from patients presenting MELAS in which ATP was decreased and bafilomycin treatment did not rise LC3B-II levels [20]. Consequently, in OXPHOS deficient cells, abnormalities in the lysosomal degradation may contribute to autophagosome and AVd accumulation.

In conclusion, in a cellular model of disease, OXPHOS deficiencies result in accumulation of autophagic vacuoles and lysosomes. This vesicular traffic-jam may interfere with normal cellular function further contributing to the disease. Future studies analyzing the regulation of autophagy-related signaling cascades in cellular models of disease, and proving the existence of similar alterations in target human tissues affected by these diseases, *i.e.*, skeletal muscle, are needed to gain insights into the disturbances of autophagy and its contribution to human OXPHOS disorders.

5. Acknowledgements

We thank Dr Sara Seneca (Center of Medical Genetics, AZ-VUB, Brussels, Belgium) for her kind gift of P4 and P5 cell lines. We thank Dr Juan Carlos González-Armas for his excellent support with the confocal microscopy and image analysis. We also thank Dr Germán Andrés for his generous gift of the antibodies against LAMP-1, GM130 and PDI. We are very grateful to the Electron Microscopy Core Facility of the Centro de Biología Molecular “Severo Ochoa” (CSIC-UAM), especially Milagros Guerra, for their skillful technical assistance. Finally, we thank Miguel Fernández Navas, Sara Jiménez and Laura Rufián for their technical assistance. This work was supported by grants PS09/01359, PI11/00182 and CP11/00151 from Instituto de Salud Carlos III (ISCIII), Ministerio de Industria y Competitividad (MINECO), Spain, S2010/BMD-2361 and S2010/BMD-2402 from Comunidad de Madrid (CAM). MAM was supported by the Programme ‘Intensificación de la actividad investigadora’, ISCIII (MINECO) and Comunidad de Madrid (Spain). AD is recipient of a research contract from ISCIII (MINECO) (PI12/01683). MM is supported by a research contract ‘Miguel Servet’ ISCIII (CP11/00151). AB is supported by a research contract (CIBERER-Spain).

6. Author Contributions

M Moran and MA Martín designed and directed the study. A Delmiro, A Blázquez and M Moran collected the samples and performed the experiments. M Moran, C Ugalde, J Arenas and MA Martín wrote the manuscript.

7. References

- [1] R.A. Nixon, The role of autophagy in neurodegenerative disease, *Nature medicine*, 19 (2013) 983-997.
- [2] I. Kissova, M. Deffieu, S. Manon, N. Camougrand, Uth1p is involved in the autophagic degradation of mitochondria, *The Journal of biological chemistry*, 279 (2004) 39068-39074.
- [3] J.J. Lemasters, Selective mitochondrial autophagy, or mitophagy, as a targeted defense against oxidative stress, mitochondrial dysfunction, and aging, *Rejuvenation research*, 8 (2005) 3-5.
- [4] S.P. Elmore, T. Qian, S.F. Grissom, J.J. Lemasters, The mitochondrial permeability transition initiates autophagy in rat hepatocytes, *FASEB journal : official publication of the Federation of American Societies for Experimental Biology*, 15 (2001) 2286-2287.
- [5] M. Priault, B. Salin, J. Schaeffer, F.M. Vallette, J.P. di Rago, J.C. Martinou, Impairing the bioenergetic status and the biogenesis of mitochondria triggers mitophagy in yeast, *Cell death and differentiation*, 12 (2005) 1613-1621.
- [6] I. Kim, S. Rodriguez-Enriquez, J.J. Lemasters, Selective degradation of mitochondria by mitophagy, *Archives of biochemistry and biophysics*, 462 (2007) 245-253.
- [7] G. Twig, A. Elorza, A.J. Molina, H. Mohamed, J.D. Wikstrom, G. Walzer, L. Stiles, S.E. Haigh, S. Katz, G. Las, J. Alroy, M. Wu, B.F. Py, J. Yuan, J.T. Deeney, B.E. Corkey, O.S. Shirihai, Fission and selective fusion govern mitochondrial segregation and elimination by autophagy, *The EMBO journal*, 27 (2008) 433-446.
- [8] D. Narendra, A. Tanaka, D.F. Suen, R.J. Youle, Parkin is recruited selectively to impaired mitochondria and promotes their autophagy, *The Journal of cell biology*, 183 (2008) 795-803.
- [9] S.L. Archer, Mitochondrial dynamics--mitochondrial fission and fusion in human diseases, *The New England journal of medicine*, 369 (2013) 2236-2251.
- [10] M.E. Gegg, J.M. Cooper, K.Y. Chau, M. Rojo, A.H. Schapira, J.W. Taanman, Mitofusin 1 and mitofusin 2 are ubiquitinated in a PINK1/parkin-dependent manner upon induction of mitophagy, *Human molecular genetics*, 19 (2010) 4861-4870.
- [11] A. Tanaka, M.M. Cleland, S. Xu, D.P. Narendra, D.F. Suen, M. Karbowski, R.J. Youle, Proteasome and p97 mediate mitophagy and degradation of mitofusins induced by Parkin, *The Journal of cell biology*, 191 (2010) 1367-1380.
- [12] C. Sauvanet, S. Duvezin-Caubet, B. Salin, C. David, A. Massoni-Laporte, J.P. di Rago, M. Rojo, Mitochondrial DNA mutations provoke dominant inhibition of mitochondrial inner membrane fusion, *PloS one*, 7 (2012) e49639.
- [13] A. Iuso, S. Scacco, C. Piccoli, F. Bellomo, V. Petruzzella, R. Trentadue, M. Minuto, M. Ripoli, N. Capitano, M. Zeviani, S. Papa, Dysfunctions of cellular oxidative metabolism in patients with mutations in the NDUFS1 and NDUFS4 genes of complex I, *The Journal of biological chemistry*, 281 (2006) 10374-10380.
- [14] R. Artuch, G. Brea-Calvo, P. Briones, A. Aracil, M. Galvan, C. Espinos, J. Corral, V. Volpini, A. Ribes, A.L. Andreu, F. Palau, J.A. Sanchez-Alcazar, P. Navas, M. Pineda, Cerebellar ataxia with coenzyme Q10 deficiency: diagnosis and follow-up after coenzyme Q10 supplementation, *Journal of the neurological sciences*, 246 (2006) 153-158.
- [15] G. Benard, N. Bellance, D. James, P. Parrone, H. Fernandez, T. Letellier, R. Rossignol, Mitochondrial bioenergetics and structural network organization, *Journal of cell science*, 120 (2007) 838-848.
- [16] A. Chevrollier, V. Guillet, D. Loiseau, N. Gueguen, M.A. de Crescenzo, C. Verny, M. Ferre, H. Dollfus, S. Odent, D. Milea, C. Goizet, P. Amati-Bonneau, V. Procaccio, D. Bonneau, P. Reynier, Hereditary optic neuropathies share a common mitochondrial coupling defect, *Annals of neurology*, 63 (2008) 794-798.
- [17] C.M. Quinzii, L.C. Lopez, J. Von-Moltke, A. Naini, S. Krishna, M. Schuelke, L. Salvati, P. Navas, S. DiMauro, M. Hirano, Respiratory chain dysfunction and oxidative stress correlate

- with severity of primary CoQ10 deficiency, *FASEB journal : official publication of the Federation of American Societies for Experimental Biology*, 22 (2008) 1874-1885.
- [18] F. Distelmaier, H.J. Visch, J.A. Smeitink, E. Mayatepek, W.J. Koopman, P.H. Willems, The antioxidant Trolox restores mitochondrial membrane potential and Ca²⁺ -stimulated ATP production in human complex I deficiency, *J Mol Med (Berl)*, 87 (2009) 515-522.
- [19] A. Rodriguez-Hernandez, M.D. Cordero, L. Salvati, R. Artuch, M. Pineda, P. Briones, L. Gomez Izquierdo, D. Cotan, P. Navas, J.A. Sanchez-Alcazar, Coenzyme Q deficiency triggers mitochondria degradation by mitophagy, *Autophagy*, 5 (2009) 19-32.
- [20] D. Cotan, M.D. Cordero, J. Garrido-Maraver, M. Oropesa-Avila, A. Rodriguez-Hernandez, L. Gomez Izquierdo, M. De la Mata, M. De Miguel, J.B. Lorite, E.R. Infante, S. Jackson, P. Navas, J.A. Sanchez-Alcazar, Secondary coenzyme Q10 deficiency triggers mitochondria degradation by mitophagy in MELAS fibroblasts, *FASEB journal : official publication of the Federation of American Societies for Experimental Biology*, 25 (2011) 2669-2687.
- [21] M. De la Mata, J. Garrido-Maraver, D. Cotan, M.D. Cordero, M. Oropesa-Avila, L.G. Izquierdo, M. De Miguel, J.B. Lorite, E.R. Infante, P. Ybot, S. Jackson, J.A. Sanchez-Alcazar, Recovery of MERRF fibroblasts and cybrids pathophysiology by Coenzyme Q(1)(0), *Neurotherapeutics : the journal of the American Society for Experimental NeuroTherapeutics*, 9 (2012) 446-463.
- [22] H. Tynismaa, K.P. Mjosund, S. Wanrooij, I. Lappalainen, E. Ylikallio, A. Jalanko, J.N. Spelbrink, A. Paetau, A. Suomalainen, Mutant mitochondrial helicase Twinkle causes multiple mtDNA deletions and a late-onset mitochondrial disease in mice, *Proceedings of the National Academy of Sciences of the United States of America*, 102 (2005) 17687-17692.
- [23] H. Tynismaa, C.J. Carroll, N. Raimundo, S. Ahola-Erkila, T. Wenz, H. Ruhanen, K. Guse, A. Hemminki, K.E. Peltola-Mjosund, V. Tulkki, M. Oresic, C.T. Moraes, K. Pietilainen, I. Hovatta, A. Suomalainen, Mitochondrial myopathy induces a starvation-like response, *Human molecular genetics*, 19 (2010) 3948-3958.
- [24] K.E. White, V.J. Davies, V.E. Hogan, M.J. Piechota, P.P. Nichols, D.M. Turnbull, M. Votruba, OPA1 deficiency associated with increased autophagy in retinal ganglion cells in a murine model of dominant optic atrophy, *Investigative ophthalmology & visual science*, 50 (2009) 2567-2571.
- [25] D. Fernandez-Moreira, C. Ugalde, R. Smeets, R.J. Rodenburg, E. Lopez-Laso, M.L. Ruiz-Falco, P. Briones, M.A. Martin, J.A. Smeitink, J. Arenas, X-linked NDUFA1 gene mutations associated with mitochondrial encephalomyopathy, *Annals of neurology*, 61 (2007) 73-83.
- [26] M. Moran, H. Rivera, M. Sanchez-Arago, A. Blazquez, B. Merinero, C. Ugalde, J. Arenas, J.M. Cuezva, M.A. Martin, Mitochondrial bioenergetics and dynamics interplay in complex I-deficient fibroblasts, *Biochimica et biophysica acta*, 1802 (2010) 443-453.
- [27] L. De Meirleir, S. Seneca, E. Damis, B. Sepulchre, A. Hoorens, E. Gerlo, M.T. Garcia Silva, E.M. Hernandez, W. Lissens, R. Van Coster, Clinical and diagnostic characteristics of complex III deficiency due to mutations in the BCS1L gene, *American journal of medical genetics. Part A*, 121A (2003) 126-131.
- [28] A. Blazquez, M.C. Gil-Borlado, M. Moran, A. Verdu, M.R. Cazorla-Calleja, M.A. Martin, J. Arenas, C. Ugalde, Infantile mitochondrial encephalomyopathy with unusual phenotype caused by a novel BCS1L mutation in an isolated complex III-deficient patient, *Neuromuscular disorders : NMD*, 19 (2009) 143-146.
- [29] M.C. Gil-Borlado, M. Gonzalez-Hoyuela, A. Blazquez, M.T. Garcia-Silva, T. Gabaldon, J. Manzanares, J. Vara, M.A. Martin, S. Seneca, J. Arenas, C. Ugalde, Pathogenic mutations in the 5' untranslated region of BCS1L mRNA in mitochondrial complex III deficiency, *Mitochondrion*, 9 (2009) 299-305.
- [30] M. Moran, L. Marin-Buera, M.C. Gil-Borlado, H. Rivera, A. Blazquez, S. Seneca, M. Vazquez-Lopez, J. Arenas, M.A. Martin, C. Ugalde, Cellular pathophysiological consequences of BCS1L mutations in mitochondrial complex III enzyme deficiency, *Human mutation*, 31 (2010) 930-941.

- [31] Y. Campos, A. Garcia-Redondo, M.A. Fernandez-Moreno, M. Martinez-Pardo, G. Goda, J.C. Rubio, M.A. Martin, P. del Hoyo, A. Cabello, B. Bornstein, R. Garesse, J. Arenas, Early-onset multisystem mitochondrial disorder caused by a nonsense mutation in the mitochondrial DNA cytochrome C oxidase II gene, *Annals of neurology*, 50 (2001) 409-413.
- [32] H. Rivera, B. Merinero, M. Martinez-Pardo, I. Arroyo, P. Ruiz-Sala, B. Bornstein, C. Serra-Suhe, E. Gallardo, R. Marti, M.J. Moran, C. Ugalde, L.A. Perez-Jurado, A.L. Andreu, R. Garesse, M. Ugarte, J. Arenas, M.A. Martin, Marked mitochondrial DNA depletion associated with a novel SUCLG1 gene mutation resulting in lethal neonatal acidosis, multi-organ failure, and interrupted aortic arch, *Mitochondrion*, 10 (2010) 362-368.
- [33] S. Kimura, N. Fujita, T. Noda, T. Yoshimori, Monitoring autophagy in mammalian cultured cells through the dynamics of LC3, *Methods in enzymology*, 452 (2009) 1-12.
- [34] M.M. Bradford, A rapid and sensitive method for the quantitation of microgram quantities of protein utilizing the principle of protein-dye binding, *Analytical biochemistry*, 72 (1976) 248-254.
- [35] S.M. Davidson, D. Yellon, M.R. Duchen, Assessing mitochondrial potential, calcium, and redox state in isolated mammalian cells using confocal microscopy, *Methods Mol Biol*, 372 (2007) 421-430.
- [36] I.A. Trounce, Y.L. Kim, A.S. Jun, D.C. Wallace, Assessment of mitochondrial oxidative phosphorylation in patient muscle biopsies, lymphoblasts, and transmitochondrial cell lines, *Methods in enzymology*, 264 (1996) 484-509.
- [37] E.L. Eskelinen, Maturation of autophagic vacuoles in Mammalian cells, *Autophagy*, 1 (2005) 1-10.
- [38] E.L. Eskelinen, Roles of LAMP-1 and LAMP-2 in lysosome biogenesis and autophagy, *Molecular aspects of medicine*, 27 (2006) 495-502.
- [39] E.L. Eskelinen, To be or not to be? Examples of incorrect identification of autophagic compartments in conventional transmission electron microscopy of mammalian cells, *Autophagy*, 4 (2008) 257-260.
- [40] P. Yla-Anttila, H. Vihinen, E. Jokitalo, E.L. Eskelinen, Monitoring autophagy by electron microscopy in Mammalian cells, *Methods in enzymology*, 452 (2009) 143-164.
- [41] D.J. Klionsky, H. Abeliovich, P. Agostinis, D.K. Agrawal, G. Aliev, D.S. Askew, M. Baba, E.H. Baehrecke, B.A. Bahr, A. Ballabio, B.A. Bamber, D.C. Bassham, E. Bergamini, X. Bi, M. Biard-Piechaczyk, J.S. Blum, D.E. Bredesen, J.L. Brodsky, J.H. Brumell, U.T. Brunk, W. Bursch, N. Camougrand, E. Cebollero, F. Cecconi, Y. Chen, L.S. Chin, A. Choi, C.T. Chu, J. Chung, P.G. Clarke, R.S. Clark, S.G. Clarke, C. Clave, J.L. Cleveland, P. Codogno, M.I. Colombo, A. Coto-Montes, J.M. Cregg, A.M. Cuervo, J. Debnath, F. Demarchi, P.B. Dennis, P.A. Dennis, V. Deretic, R.J. Devenish, F. Di Sano, J.F. Dice, M. Difiglia, S. Dinesh-Kumar, C.W. Distelhorst, M. Djavaheri-Mergny, F.C. Dorsey, W. Droge, M. Dron, W.A. Dunn, Jr., M. Duszenko, N.T. Eissa, Z. Elazar, A. Esclatine, E.L. Eskelinen, L. Fesus, K.D. Finley, J.M. Fuentes, J. Fueyo, K. Fujisaki, B. Galliot, F.B. Gao, D.A. Gewirtz, S.B. Gibson, A. Gohla, A.L. Goldberg, R. Gonzalez, C. Gonzalez-Estevez, S. Gorski, R.A. Gottlieb, D. Haussinger, Y.W. He, K. Heidenreich, J.A. Hill, M. Hoyer-Hansen, X. Hu, W.P. Huang, A. Iwasaki, M. Jaattela, W.T. Jackson, X. Jiang, S. Jin, T. Johansen, J.U. Jung, M. Kadowaki, C. Kang, A. Kelekar, D.H. Kessel, J.A. Kiel, H.P. Kim, A. Kimchi, T.J. Kinsella, K. Kiselyov, K. Kitamoto, E. Knecht, M. Komatsu, E. Kominami, S. Kondo, A.L. Kovacs, G. Kroemer, C.Y. Kuan, R. Kumar, M. Kundu, J. Landry, M. Laporte, W. Le, H.Y. Lei, M.J. Lenardo, B. Levine, A. Lieberman, K.L. Lim, F.C. Lin, W. Liou, L.F. Liu, G. Lopez-Berestein, C. Lopez-Otin, B. Lu, K.F. Macleod, W. Malorni, W. Martinet, K. Matsuoka, J. Mautner, A.J. Meijer, A. Melendez, P. Michels, G. Miotto, W.P. Mistiaen, N. Mizushima, B. Mograbi, I. Monastyrska, M.N. Moore, P.I. Moreira, Y. Moriyasu, T. Motyl, C. Munz, L.O. Murphy, N.I. Naqvi, T.P. Neufeld, I. Nishino, R.A. Nixon, T. Noda, B. Nurnberg, M. Ogawa, N.L. Oleinick, L.J. Olsen, B. Ozpolat, S. Paglin, G.E. Palmer, I. Papassideri, M. Parkes, D.H. Perlmutter, G. Perry, M. Piacentini, R. Pinkas-Kramarski, M. Prescott, T. Proikas-Cezanne, N. Raben, A. Rami, F. Reggiori, B. Rohrer, D.C. Rubinsztein, K.M. Ryan, J. Sadoshima, H. Sakagami, Y. Sakai, M. Sandri, C. Sasakawa, M. Sass, C. Schneider,

689 P.O. Seglen, O. Seleverstov, J. Settleman, J.J. Shacka, I.M. Shapiro, A. Sibirny, E.C. Silva-Zacarin,
 690 H.U. Simon, C. Simone, A. Simonsen, M.A. Smith, K. Spaniel-Borowski, V. Srinivas, M. Steeves,
 691 H. Stenmark, P.E. Stromhaug, C.S. Subauste, S. Sugimoto, D. Sulzer, T. Suzuki, M.S. Swanson, I.
 692 Tabas, F. Takeshita, N.J. Talbot, Z. Talloczy, K. Tanaka, I. Tanida, G.S. Taylor, J.P. Taylor, A.
 693 Terman, G. Tettamanti, C.B. Thompson, M. Thumm, A.M. Tolkovsky, S.A. Tooze, R. Truant, L.V.
 694 Tumanovska, Y. Uchiyama, T. Ueno, N.L. Uzcategui, I. van der Klei, E.C. Vaquero, T. Vellai, M.W.
 695 Vogel, H.G. Wang, P. Webster, J.W. Wiley, Z. Xi, G. Xiao, J. Yahalom, J.M. Yang, G. Yap, X.M. Yin,
 696 T. Yoshimori, L. Yu, Z. Yue, M. Yuzaki, O. Zabirnyk, X. Zheng, X. Zhu, R.L. Deter, Guidelines for
 697 the use and interpretation of assays for monitoring autophagy in higher eukaryotes,
 698 *Autophagy*, 4 (2008) 151-175.
 699 [42] D.P. Narendra, S.M. Jin, A. Tanaka, D.F. Suen, C.A. Gautier, J. Shen, M.R. Cookson, R.J.
 700 Youle, PINK1 is selectively stabilized on impaired mitochondria to activate Parkin, *PLoS biology*,
 701 8 (2010) e1000298.
 702 [43] R.W. Gilkerson, R.L. De Vries, P. Lebot, J.D. Wikstrom, E. Torgykes, O.S. Shirihai, S.
 703 Przedborski, E.A. Schon, Mitochondrial autophagy in cells with mtDNA mutations results from
 704 synergistic loss of transmembrane potential and mTORC1 inhibition, *Human molecular*
 705 *genetics*, 21 (2012) 978-990.
 706 [44] M. Deffieu, I. Bhatia-Kissova, B. Salin, D.J. Klionsky, B. Pinson, S. Manon, N. Camougrand,
 707 Increased levels of reduced cytochrome b and mitophagy components are required to trigger
 708 nonspecific autophagy following induced mitochondrial dysfunction, *Journal of cell science*,
 709 126 (2013) 415-426.
 710 [45] D. Tondera, S. Grandemange, A. Jourdain, M. Karbowski, Y. Mattenberger, S. Herzig, S. Da
 711 Cruz, P. Clerc, I. Raschke, C. Merkwirth, S. Ehses, F. Krause, D.C. Chan, C. Alexander, C. Bauer,
 712 R. Youle, T. Langer, J.C. Martinou, SLP-2 is required for stress-induced mitochondrial
 713 hyperfusion, *The EMBO journal*, 28 (2009) 1589-1600.
 714 [46] K. Mitra, C. Wunder, B. Roysam, G. Lin, J. Lippincott-Schwartz, A hyperfused mitochondrial
 715 state achieved at G1-S regulates cyclin E buildup and entry into S phase, *Proceedings of the*
 716 *National Academy of Sciences of the United States of America*, 106 (2009) 11960-11965.
 717 [47] L.C. Gomes, G. Di Benedetto, L. Scorrano, During autophagy mitochondria elongate, are
 718 spared from degradation and sustain cell viability, *Nature cell biology*, 13 (2011) 589-598.
 719 [48] D. Narendra, A. Tanaka, D.F. Suen, R.J. Youle, Parkin-induced mitophagy in the
 720 pathogenesis of Parkinson disease, *Autophagy*, 5 (2009) 706-708.
 721 [49] D. Narendra, L.A. Kane, D.N. Hauser, I.M. Fearnley, R.J. Youle, p62/SQSTM1 is required for
 722 Parkin-induced mitochondrial clustering but not mitophagy; VDAC1 is dispensable for both,
 723 *Autophagy*, 6 (2010) 1090-1106.
 724 [50] C. Vives-Bauza, C. Zhou, Y. Huang, M. Cui, R.L. de Vries, J. Kim, J. May, M.A. Tocilescu, W.
 725 Liu, H.S. Ko, J. Magrane, D.J. Moore, V.L. Dawson, R. Grailhe, T.M. Dawson, C. Li, K. Tieu, S.
 726 Przedborski, PINK1-dependent recruitment of Parkin to mitochondria in mitophagy,
 727 *Proceedings of the National Academy of Sciences of the United States of America*, 107 (2010)
 728 378-383.
 729 [51] V.S. Van Laar, B. Arnold, S.J. Cassady, C.T. Chu, E.A. Burton, S.B. Berman, Bioenergetics of
 730 neurons inhibit the translocation response of Parkin following rapid mitochondrial
 731 depolarization, *Human molecular genetics*, 20 (2011) 927-940.
 732 [52] A. Rakovic, A. Grunewald, P. Seibler, A. Ramirez, N. Kock, S. Orolicki, K. Lohmann, C. Klein,
 733 Effect of endogenous mutant and wild-type PINK1 on Parkin in fibroblasts from Parkinson
 734 disease patients, *Human molecular genetics*, 19 (2010) 3124-3137.
 735 [53] F.H. Sterky, S. Lee, R. Wibom, L. Olson, N.G. Larsson, Impaired mitochondrial transport and
 736 Parkin-independent degeneration of respiratory chain-deficient dopamine neurons in vivo,
 737 *Proceedings of the National Academy of Sciences of the United States of America*, 108 (2011)
 738 12937-12942.

- [54] F. Darios, O. Corti, C.B. Lucking, C. Hampe, M.P. Muriel, N. Abbas, W.J. Gu, E.C. Hirsch, T. Rooney, M. Ruberg, A. Brice, Parkin prevents mitochondrial swelling and cytochrome c release in mitochondria-dependent cell death, *Human molecular genetics*, 12 (2003) 517-526.
- [55] Y. Kuroda, T. Mitsui, M. Kunishige, M. Shono, M. Akaike, H. Azuma, T. Matsumoto, Parkin enhances mitochondrial biogenesis in proliferating cells, *Human molecular genetics*, 15 (2006) 883-895.
- [56] O. Rothfuss, H. Fischer, T. Hasegawa, M. Maisel, P. Leitner, F. Miesel, M. Sharma, A. Bornemann, D. Berg, T. Gasser, N. Patenge, Parkin protects mitochondrial genome integrity and supports mitochondrial DNA repair, *Human molecular genetics*, 18 (2009) 3832-3850.
- [57] Y. Kuroda, W. Sako, S. Goto, T. Sawada, D. Uchida, Y. Izumi, T. Takahashi, N. Kagawa, M. Matsumoto, R. Takahashi, R. Kaji, T. Mitsui, Parkin interacts with Klok1 for mitochondrial import and maintenance of membrane potential, *Human molecular genetics*, 21 (2012) 991-1003.
- [58] E.S. Vincow, G. Merrihew, R.E. Thomas, N.J. Shulman, R.P. Beyer, M.J. MacCoss, L.J. Pallanck, The PINK1-Parkin pathway promotes both mitophagy and selective respiratory chain turnover in vivo, *Proceedings of the National Academy of Sciences of the United States of America*, 110 (2013) 6400-6405.
- [59] C.H. Huang, M. Lazarou, R.J. Youle, Sequestration and autophagy of mitochondria do not cut proteins across the board, *Proceedings of the National Academy of Sciences of the United States of America*, 110 (2013) 6252-6253.
- [60] S.W. Suzuki, J. Onodera, Y. Ohsumi, Starvation induced cell death in autophagy-defective yeast mutants is caused by mitochondria dysfunction, *PloS one*, 6 (2011) e17412.
- [61] H. Kotarsky, M. Keller, M. Davoudi, P. Leveen, R. Karikoski, D.P. Enot, V. Fellman, Metabolite profiles reveal energy failure and impaired beta-oxidation in liver of mice with complex III deficiency due to a BCS1L mutation, *PloS one*, 7 (2012) e41156.
- [62] J.H. Yuan, Y. Sakiyama, I. Higuchi, Y. Inamori, Y. Higuchi, A. Hashiguchi, K. Higashi, A. Yoshimura, H. Takashima, Mitochondrial myopathy with autophagic vacuoles in patients with the m.8344A>G mutation, *Journal of clinical pathology*, 66 (2013) 659-664.
- [63] L. Yu, C.K. McPhee, L. Zheng, G.A. Mardones, Y. Rong, J. Peng, N. Mi, Y. Zhao, Z. Liu, F. Wan, D.W. Hailey, V. Oorschot, J. Klumperman, E.H. Baehrecke, M.J. Lenardo, Termination of autophagy and reformation of lysosomes regulated by mTOR, *Nature*, 465 (2010) 942-946.
- [64] M. Graef, J. Nunnari, Mitochondria regulate autophagy by conserved signalling pathways, *The EMBO journal*, 30 (2011) 2101-2114.
- [65] M. Sakai, K. Ogawa, Energy-dependent lysosomal wrapping mechanism (LWM) during autophagolysosome formation, *Histochemistry*, 76 (1982) 479-488.
- [66] P.J. Plomp, E.J. Wolvetang, A.K. Groen, A.J. Meijer, P.B. Gordon, P.O. Seglen, Energy dependence of autophagic protein degradation in isolated rat hepatocytes, *European journal of biochemistry / FEBS*, 164 (1987) 197-203.
- [67] J.P. Schellens, A.J. Meijer, Energy depletion and autophagy. Cytochemical and biochemical studies in isolated rat hepatocytes, *The Histochemical journal*, 23 (1991) 460-466.
- [68] A.L. Kovacs, P.B. Gordon, E.M. Grotterod, P.O. Seglen, Inhibition of hepatocytic autophagy by adenosine, adenosine analogs and AMP, *Biological chemistry*, 379 (1998) 1341-1347.
- [69] J.F. Moruno-Manchon, E. Perez-Jimenez, E. Knecht, Glucose induces autophagy under starvation conditions by a p38 MAPK-dependent pathway, *The Biochemical journal*, 449 (2013) 497-506.

8. Figure Legends

Figure 1. A) Mitochondrial membrane potential determined by confocal microscopy expressed as mean TMRM fluorescence per cell normalized by citrate synthase activity in control fibroblasts (C) and fibroblasts from patients with isolated complex I deficiency (P1-P3), complex III deficiency (P4-P8), complex IV deficiency (P9, P10) and decreased mtDNA content (P11). Data presented are mean \pm SD (n=3-8). Four different controls were analyzed. Kruskal Wallis test: significant cell line effect ($P = 0.047$). * $P < 0.05$ significantly different of C. B) ATP content in controls (C), and cells showing complex III deficiency (P4-P8) and decreased mtDNA content (P11). Data are presented as mean \pm SD (n=3-5). Four control cell lines were analyzed. Mann-Whitney test $P = 0.01$ for patients vs. controls.

Figure 2. Immunofluorescence to detect the autophagosomal marker LC3B (green) and the mitochondrial marker complex V α subunit (red) in control fibroblasts (C) and fibroblasts from patients with isolated complex I deficiency (P1-P3), complex III deficiency (P4-P8), complex IV deficiency (P9, P10) and decreased mtDNA content (P11). Colocalized pixels are shown in white. P6 Inset: enlarged area showing colocalization of small fragmented mitochondria and autophagosomes. Five different controls were analyzed. 63x Plan-Apochromat objective.

Figure 3. A) Western blot analysis of complex V α subunit (CV α) in control fibroblasts (C) and fibroblasts from patients with isolated complex I deficiency (P1-P3), complex III deficiency (P4-P8), complex IV deficiency (P9, P10), and decreased mtDNA content (P11). β -actin was used as loading control. B) Levels of the key mitochondrial proteins, complex II 70 kDa subunit (SDHA) and pyruvate dehydrogenase E1- α subunit (PDH-E1- α) in control fibroblasts (C) and fibroblasts from patients with isolated complex I deficiency (P1-P3), complex III deficiency (P4-P8), complex IV deficiency (P9, P10), and decreased mtDNA content (P11). α -tubulin was used as loading control. C) Representative western blot against SDHA, CV α , PDH-E1- α in six different

control cell lines (C1-C6) and complex I and complex III-deficient cells (P1, P4) with their respective loading controls (β -actin for SDHA and CV α , and α -tubulin for PDH-E1- α).

Figure 4. Immunofluorescence to detect Parkin (green) and the mitochondrial marker complex V α subunit (red) in control fibroblasts (C) and fibroblasts from patients with isolated complex I deficiency (P1-P3), complex III deficiency (P4-P8), complex IV deficiency (P9, P10), and decreased mtDNA content (P11). Colocalized pixels are shown in white. Four different controls were analyzed. 63x Plan-Apochromat objective.

Figure 5. A) LC3B levels in human fibroblasts from patients with isolated complex I deficiency (P1-P3), complex III deficiency (P4-P8), complex IV deficiency (P9, P10), and decreased mtDNA content (P11). β -actin was used as loading control. B) Analysis of the densitometry LC3B-II/actin ratio, data are presented as mean \pm SD (n=3-5). Five different controls were analyzed. Mann-Whitney test $P = 0.013$ for patients vs. controls. C) Representative western blot against LC3B in six different controls (C1-C6) and complex I and complex III-deficient cells (P1, P4). β -actin was used as loading control.

Figure 6. Autophagic flux in cells treated with lysosomal protease inhibitors E64D and Pepstatin A (+), or vehicle treated (-). A) Representative western blot to detect LC3B in control fibroblasts (C) and fibroblast from MD patients with isolated complex I deficiency (P1-P3), complex III deficiency (P4-P8), complex IV deficiency (P9, P10), and decreased mtDNA content (P11). β -actin was used as loading control. Please, note that loading was decreased in patients' cells to avoid saturation. B) Analysis of the densitometry of the LC3B-II/actin ratio, data are presented as mean \pm SD (n=3-5). Four different controls were analyzed. Mann-Whitney test did not show significant differences for patients vs. controls.

Figure 7. A) Electron microscopy of ultrathin sections of control fibroblasts (C) and fibroblasts derived from MD patients with isolated complex I deficiency (P1-P3), complex III deficiency (P5, P6, P8), complex IV deficiency (P9), and decreased mtDNA content (P11). Examples of late

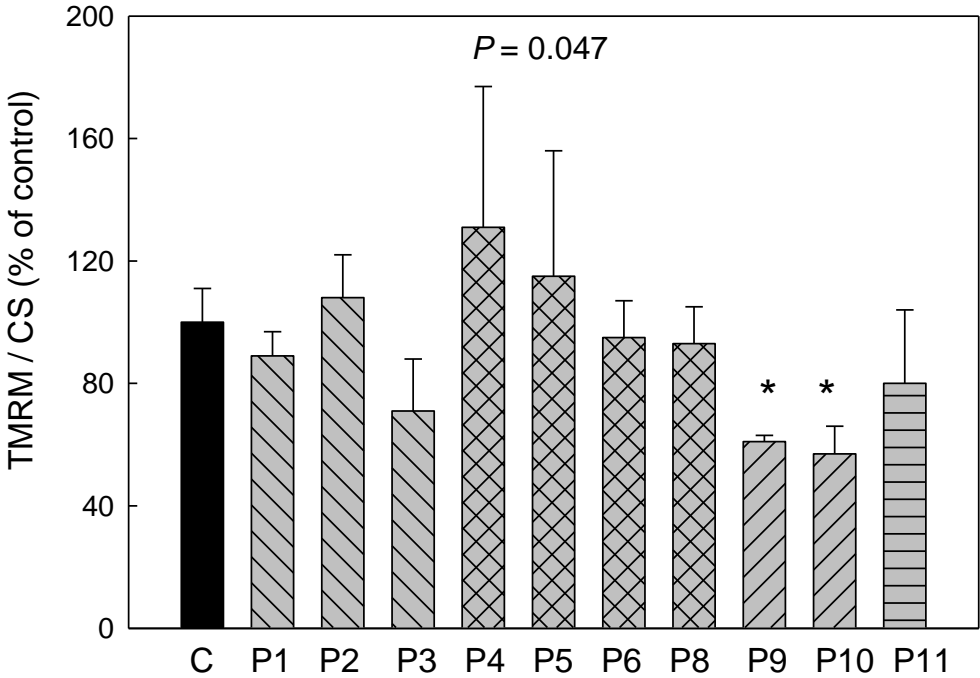
or degradative autophagic vacuoles (AVd) are depicted by arrowheads. Images shown are tiling of 2x3 or 3x3, 8K individual images. B) Stereological counting of AVd expressed as AVd/μ^2 , data are presented as mean \pm SD. Four different controls were analyzed. Mann-Whitney test $P < 0.01$ for patients vs. controls.

Figure 8. A) Lysosomal protein LAMP-1 levels in control fibroblasts (C) and fibroblasts from patients with isolated complex I deficiency (P1-P3), complex III deficiency (P4-P8), complex IV deficiency (P9, P10), and decreased mtDNA content (P11). β -actin was used as loading control. B) Analysis of the densitometry LAMP-1/actin ratio, data are presented as mean \pm SD (n=3-5). Four different controls were analyzed. Mann-Whitney test $P = 0.016$ for patients vs controls. C) Representative western blot against LAMP-1 in six different control cell lines (C1-C6) and complex I and complex III-deficient cells (P1, P4). β -actin was used as loading control.

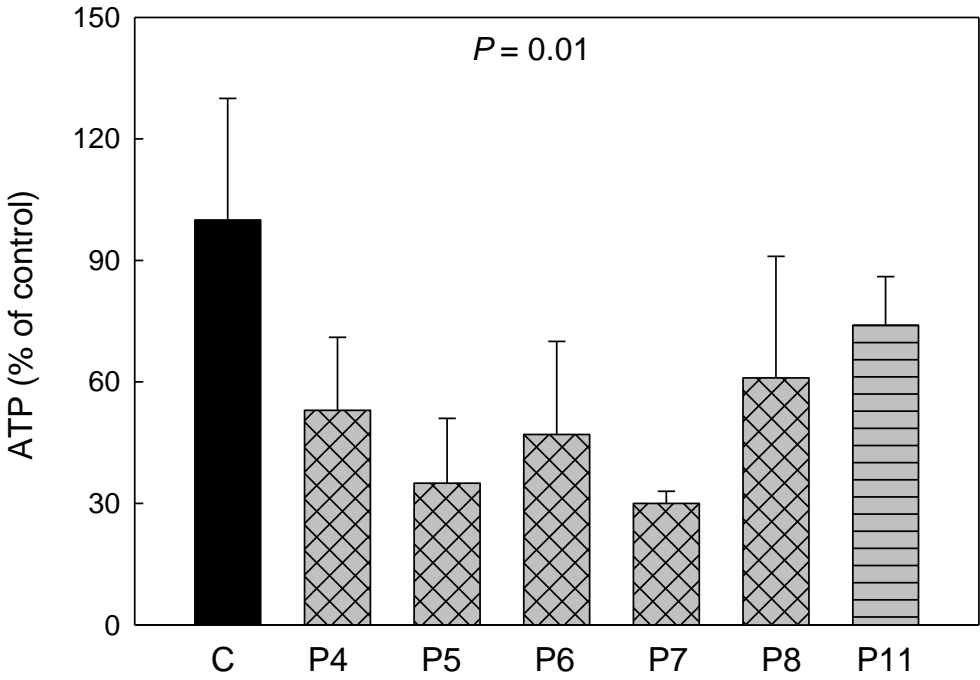
Figure 9. A) Lysosomal content in living cells stained with Lysotracker® DND-26: control fibroblasts (C), fibroblasts from patients with isolated complex I deficiency (P1,P2), complex III deficiency (P4-P8), complex IV deficiency (P9), and decreased mtDNA content (P11). Cells were viewed with a Zeiss LSM 510 Meta confocal microscope with a 40x Plan-Neofluar objective. B) Quantitative analysis of Lysotracker® DND-26 staining intensity in control (C) and MD cells (P1-P11). Four different controls were analyzed. Mann-Whitney test $P=0.007$ for patients vs. controls.

Figure 1

A



B



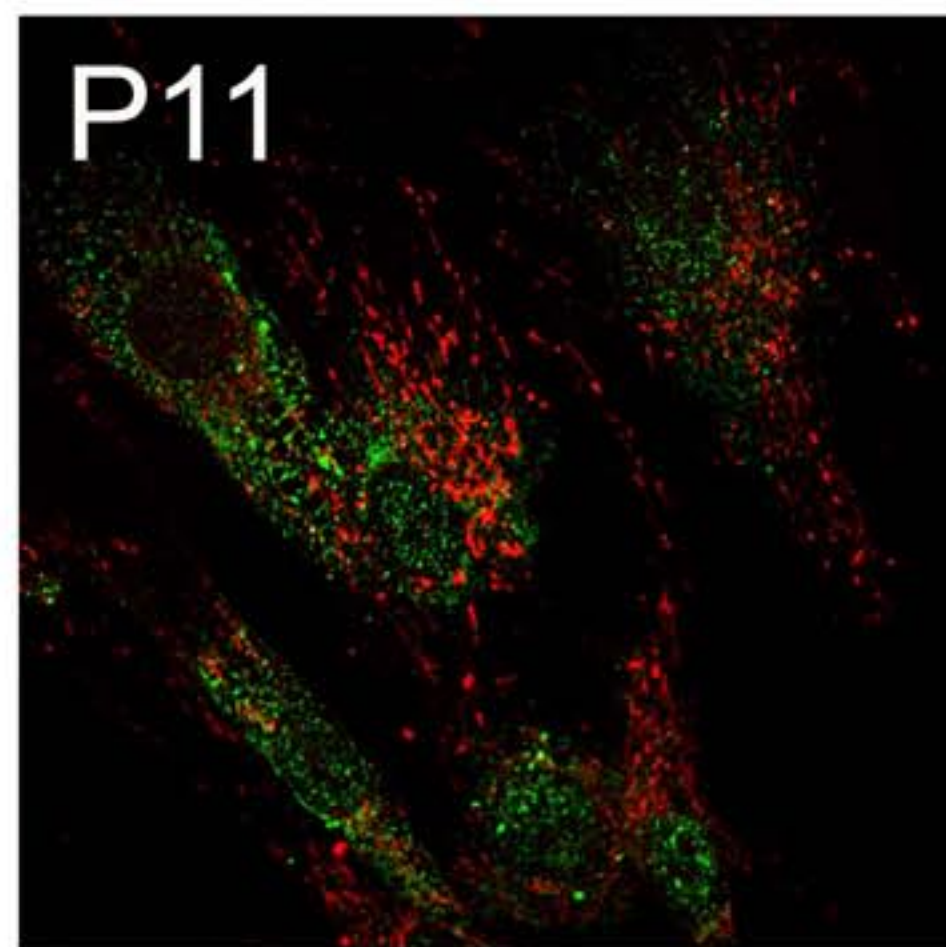
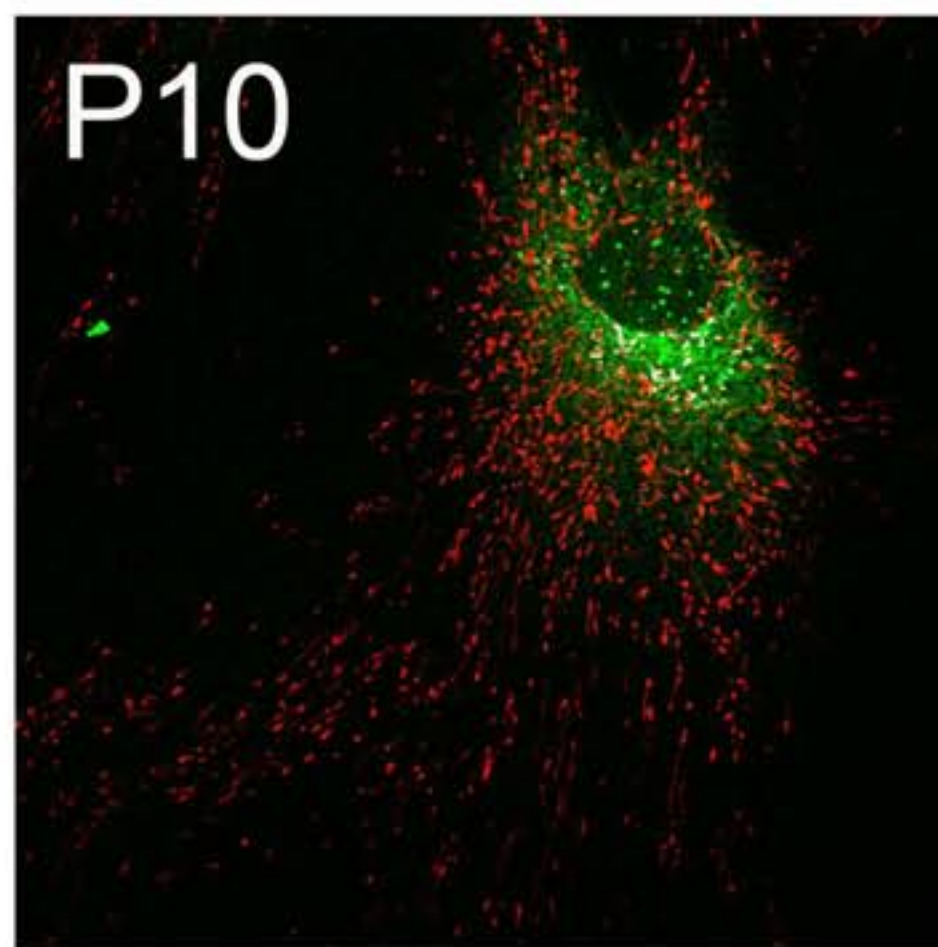
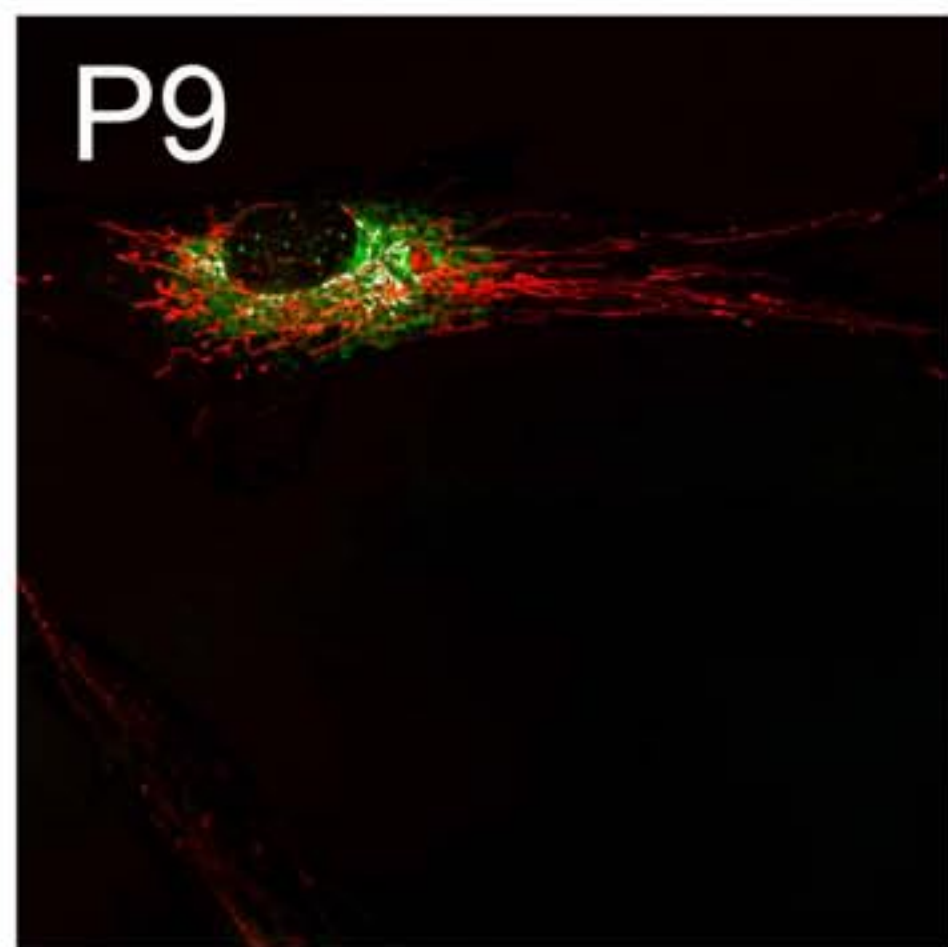
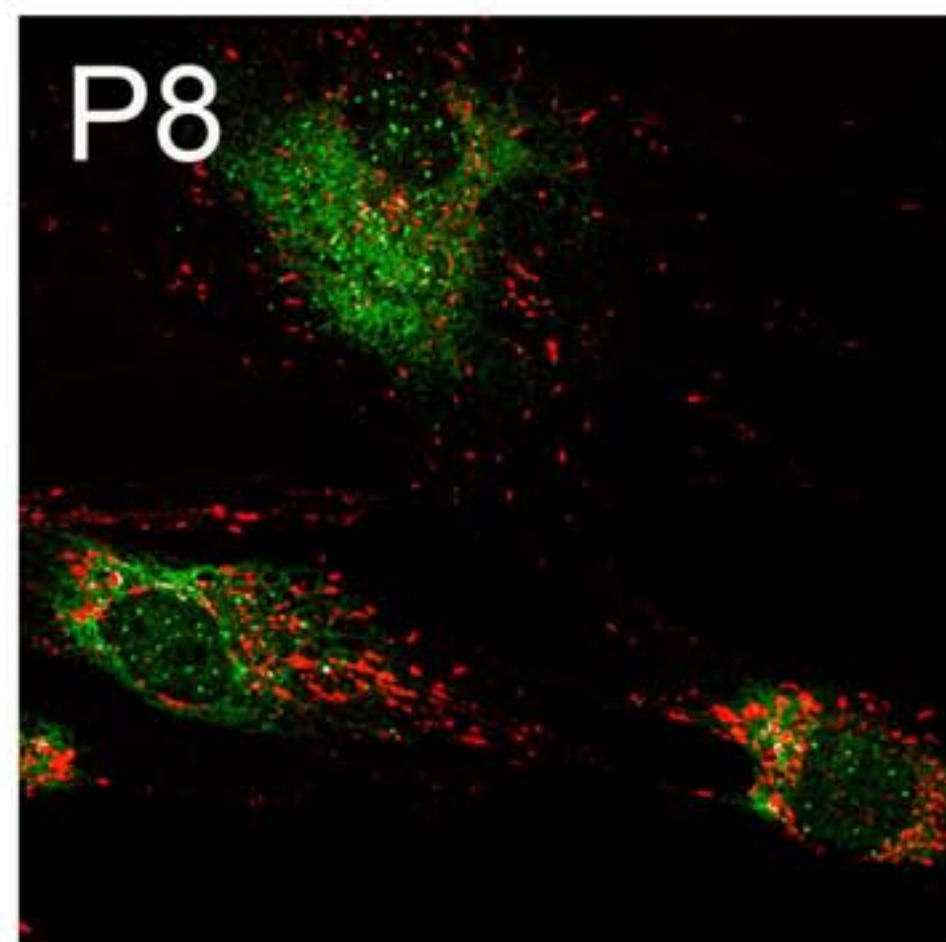
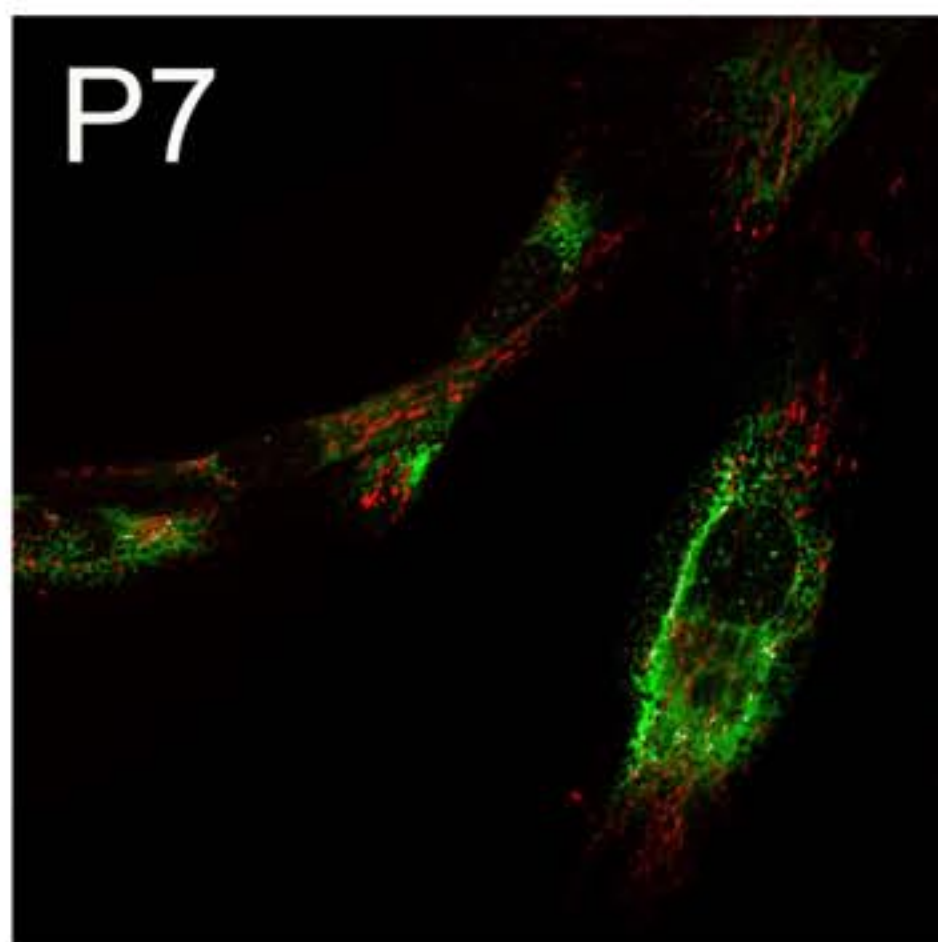
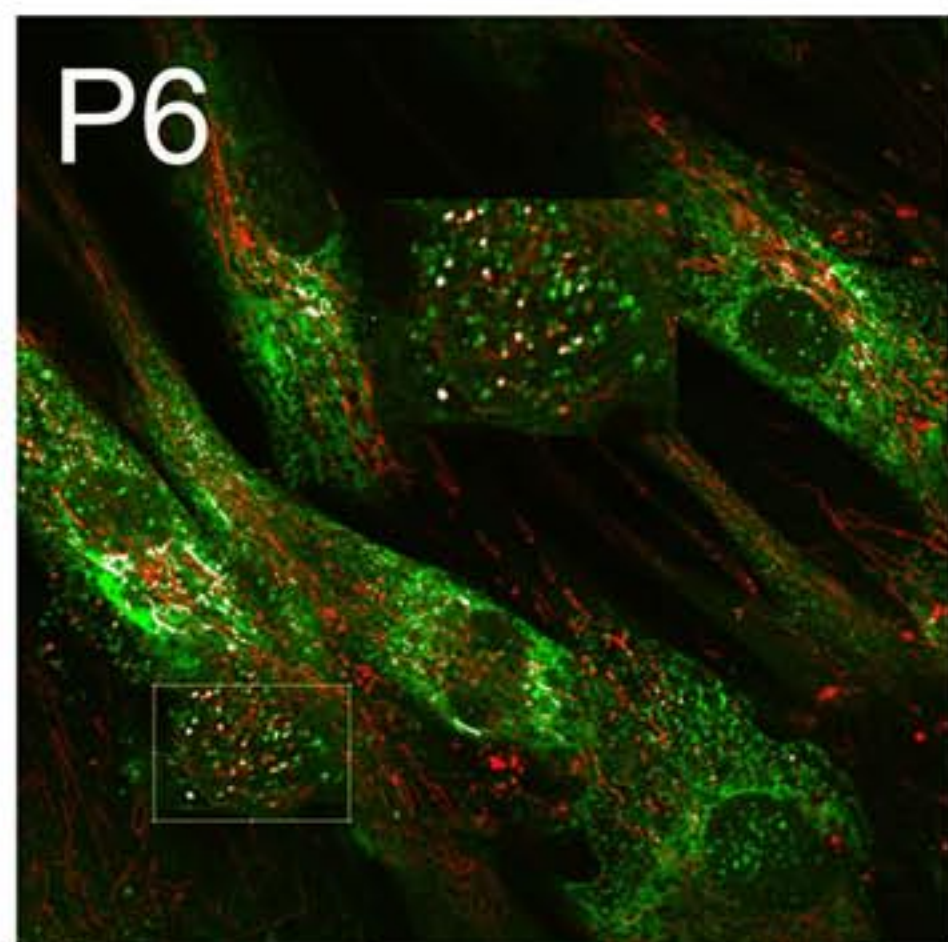
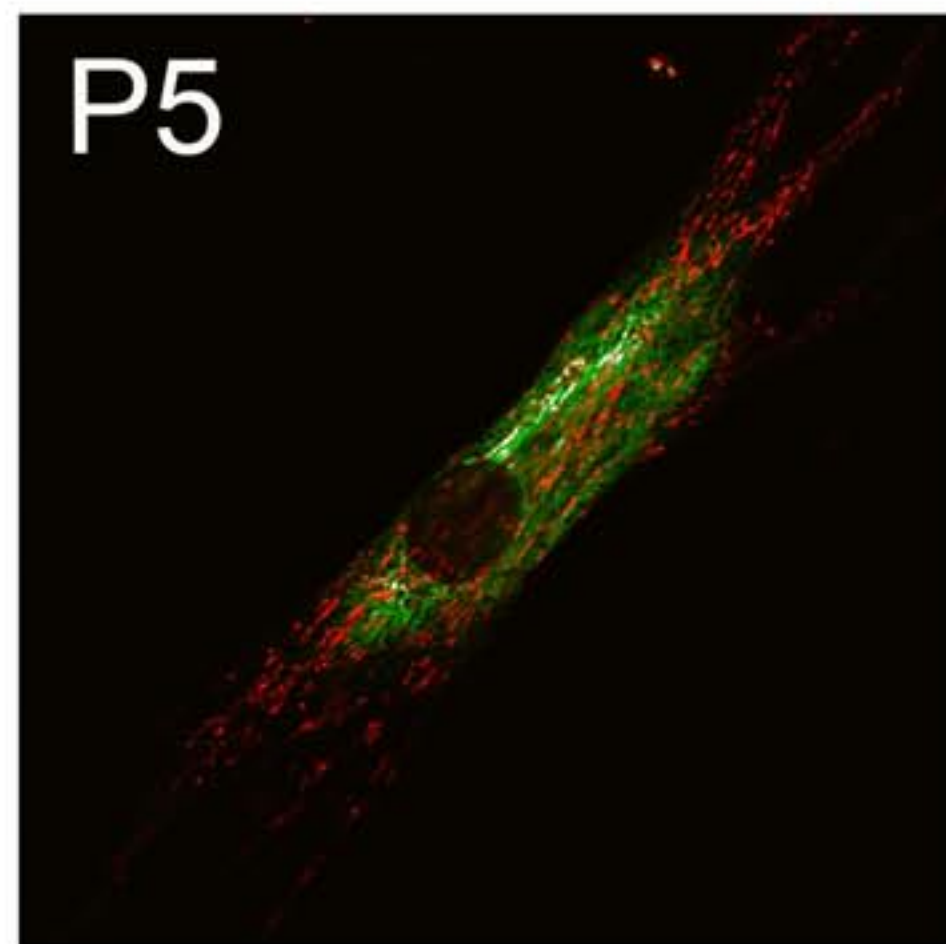
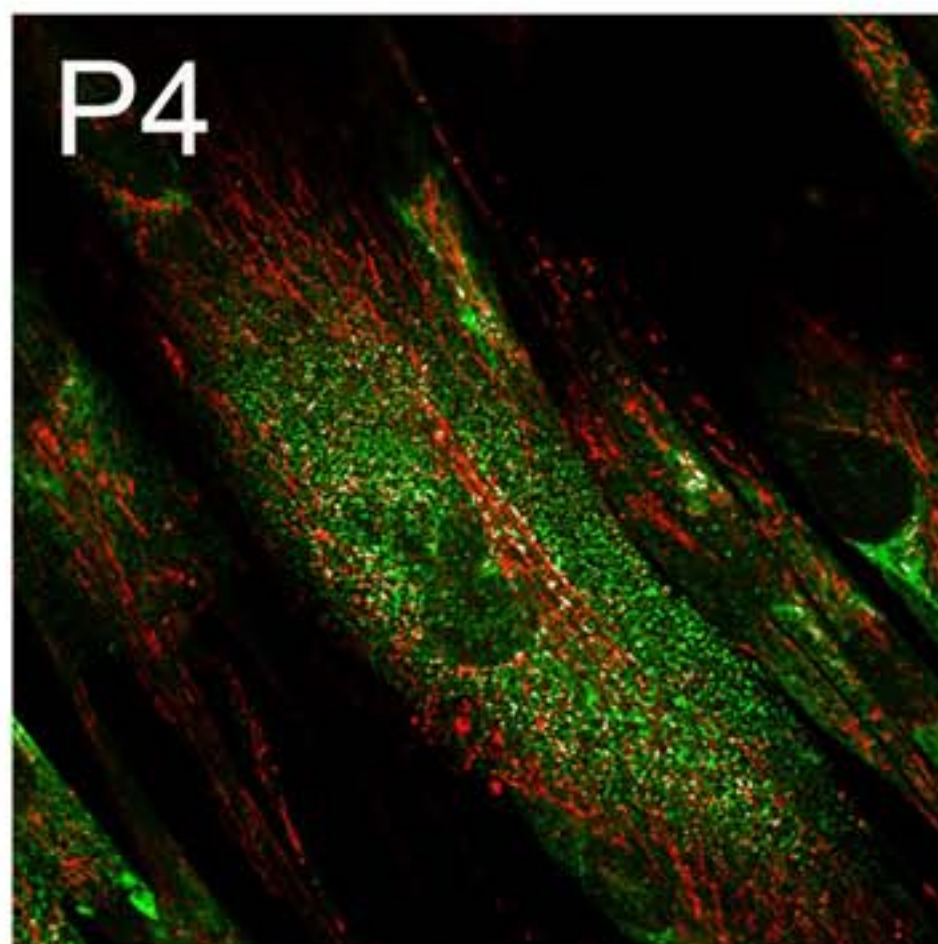
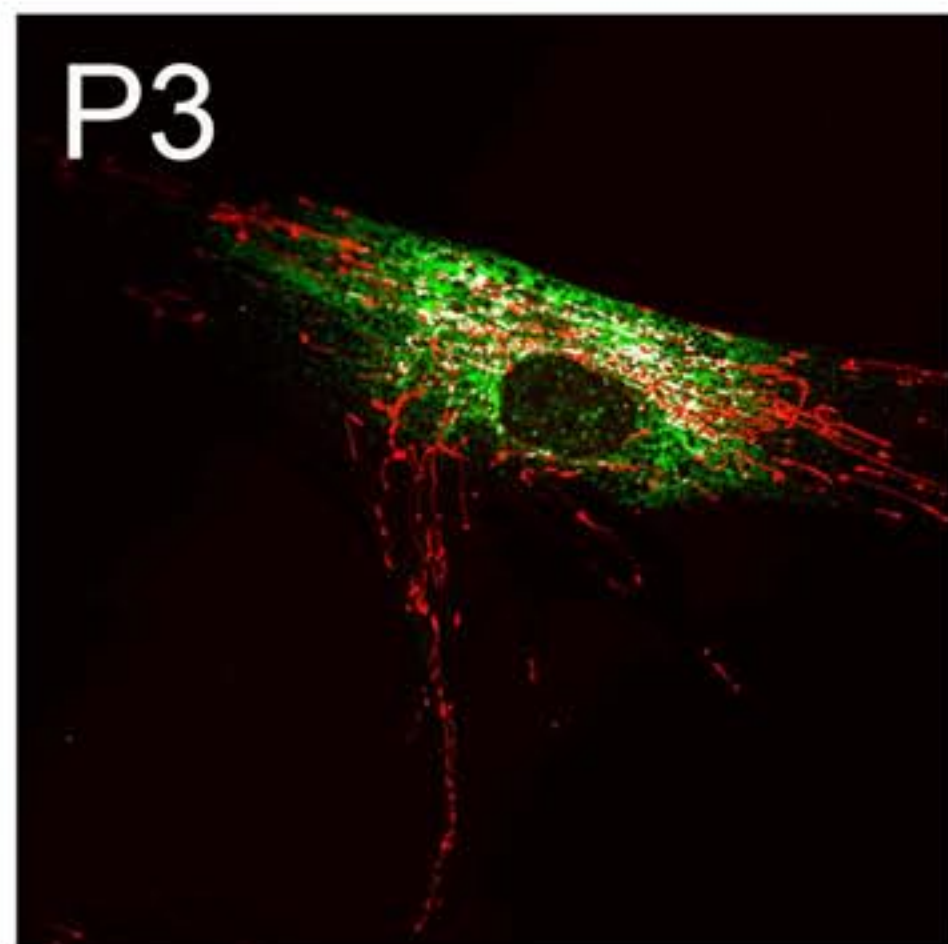
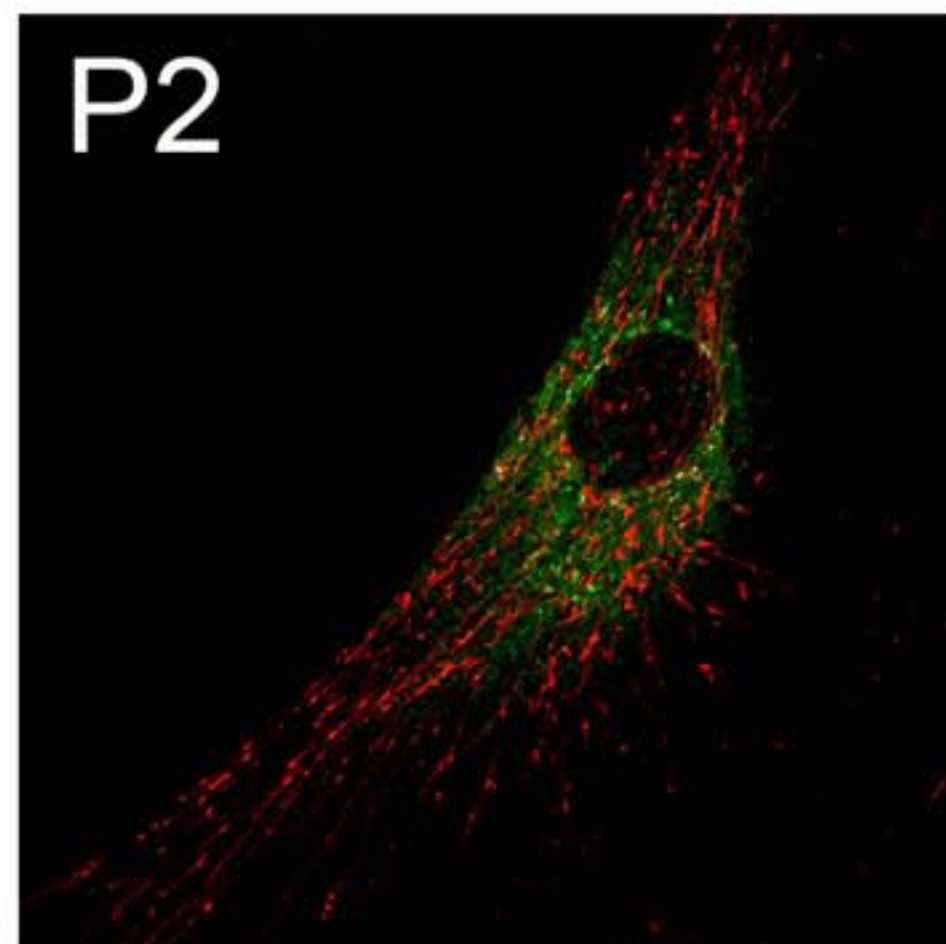
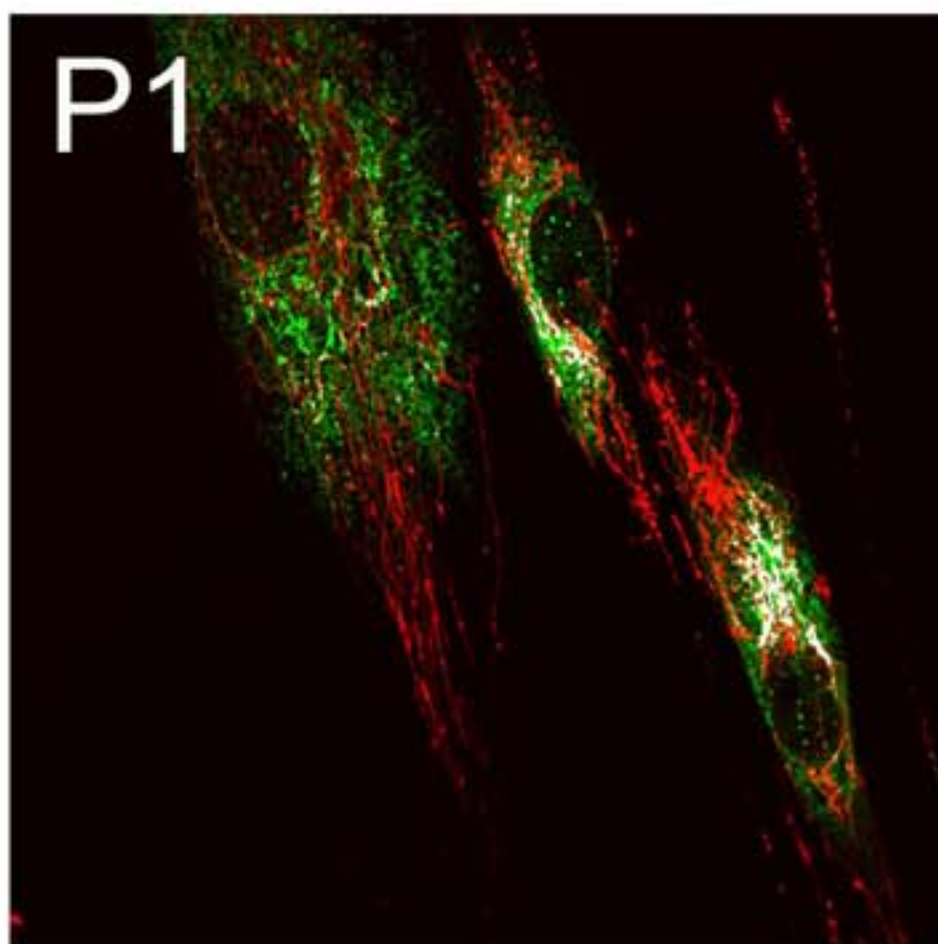
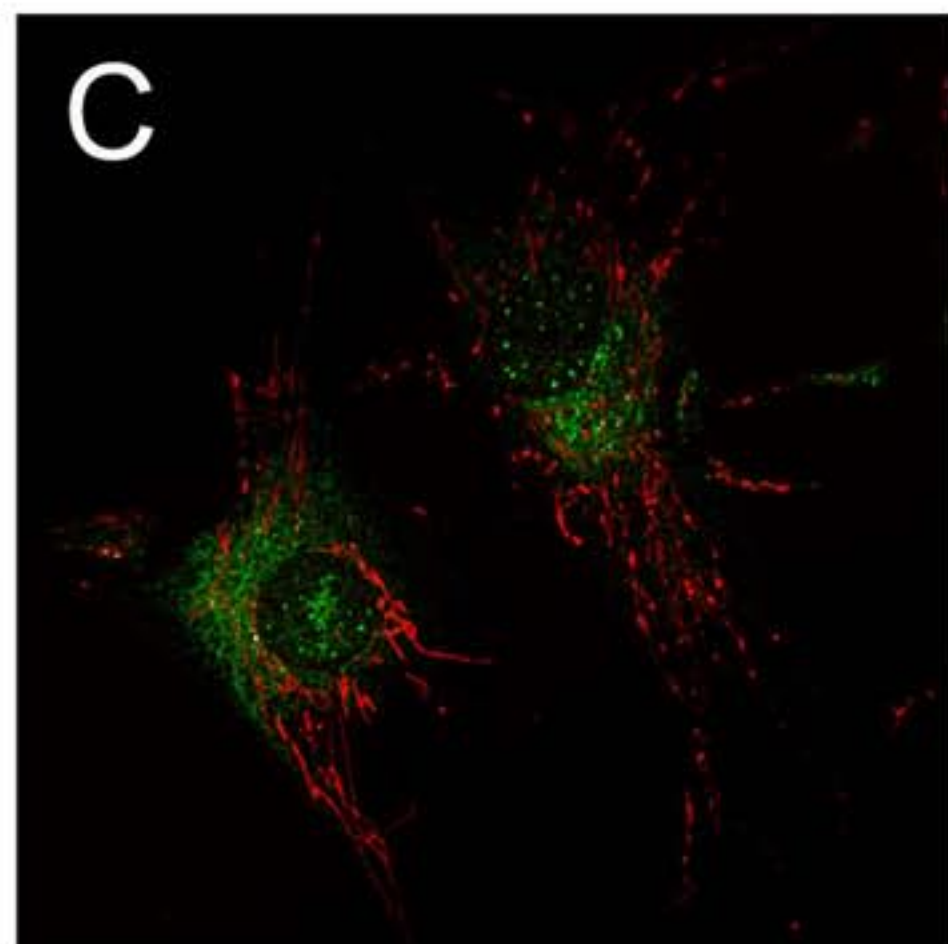
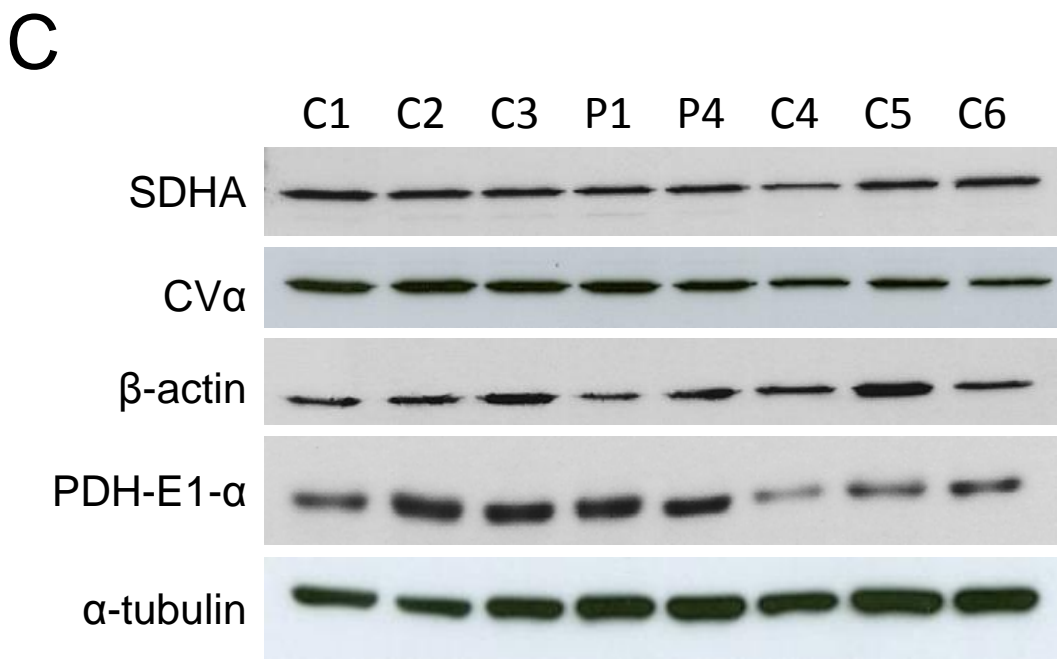
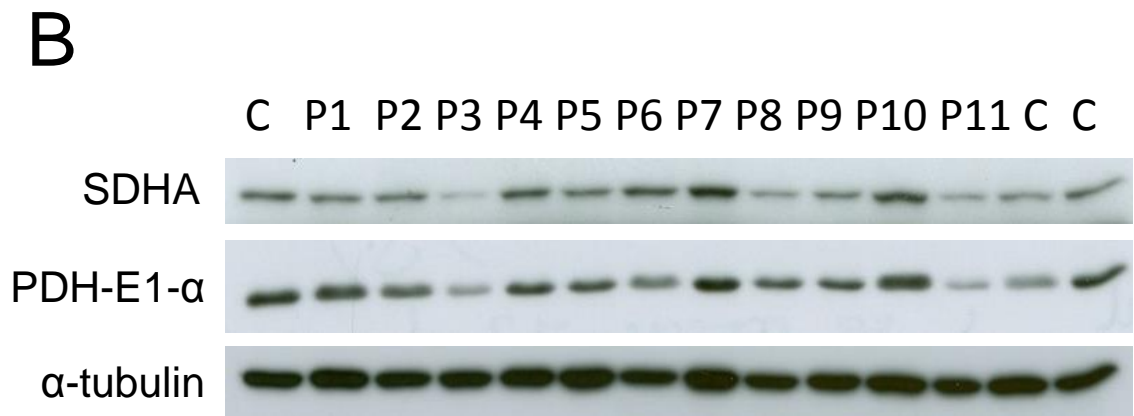
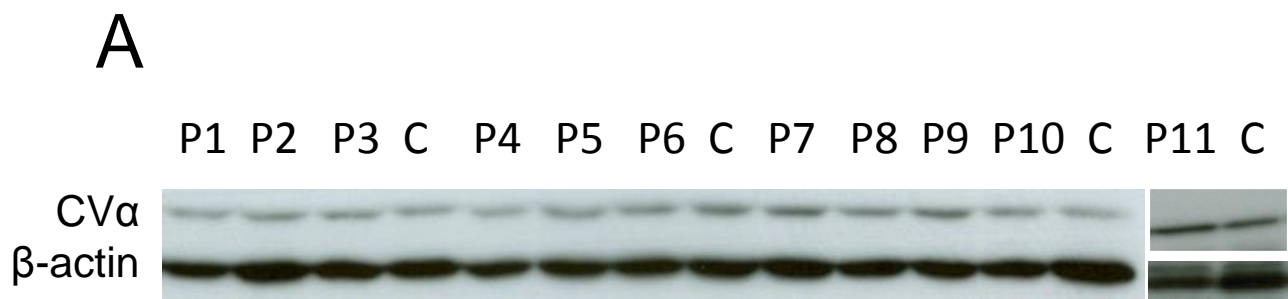


Figure 3



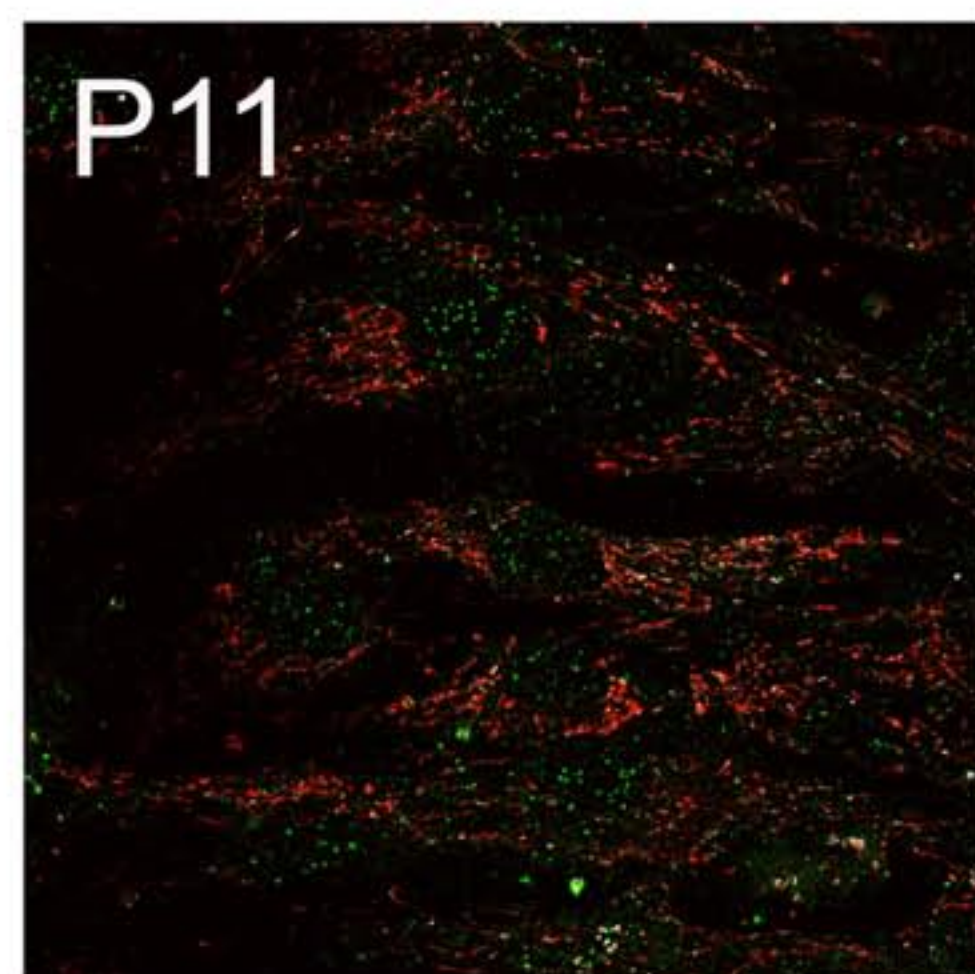
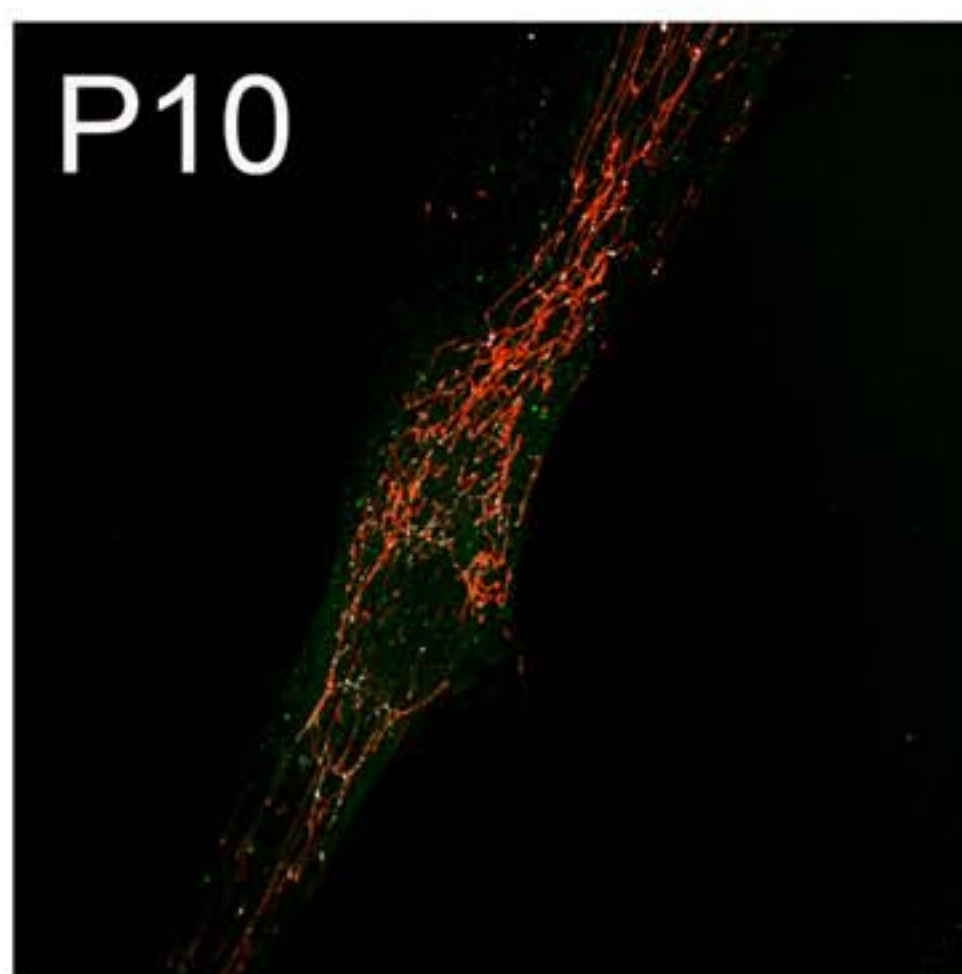
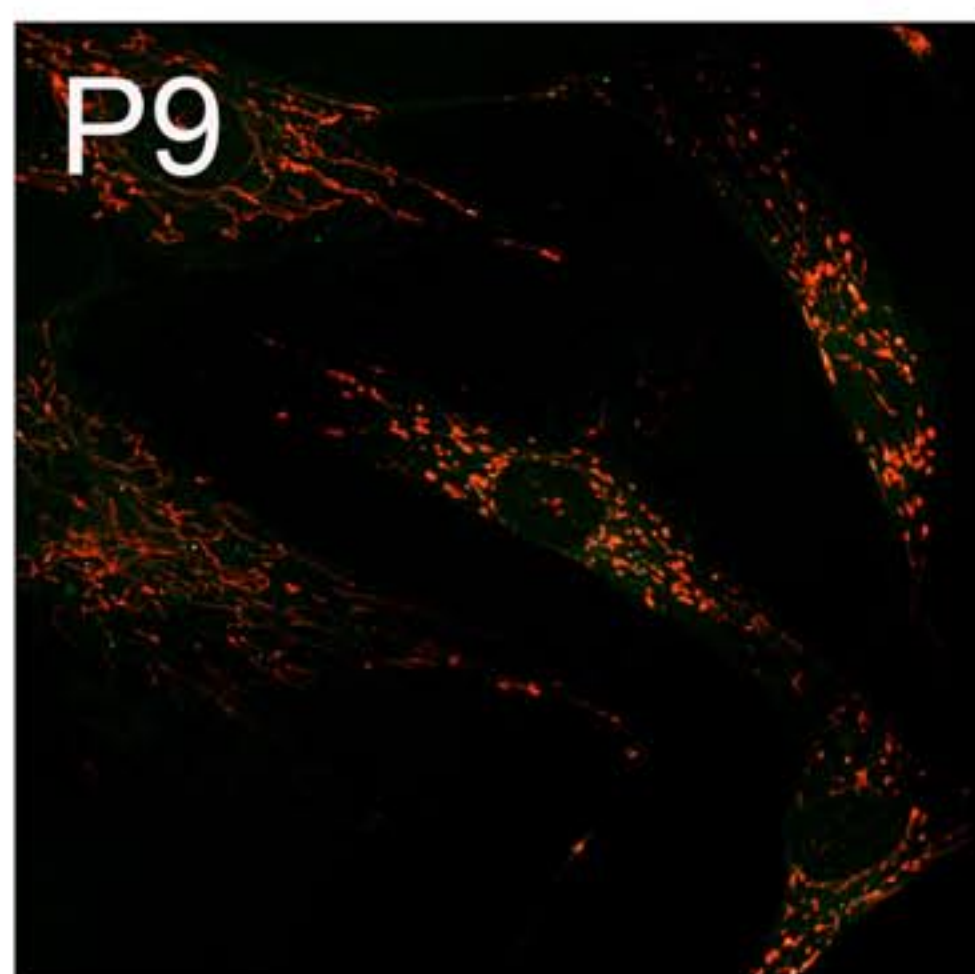
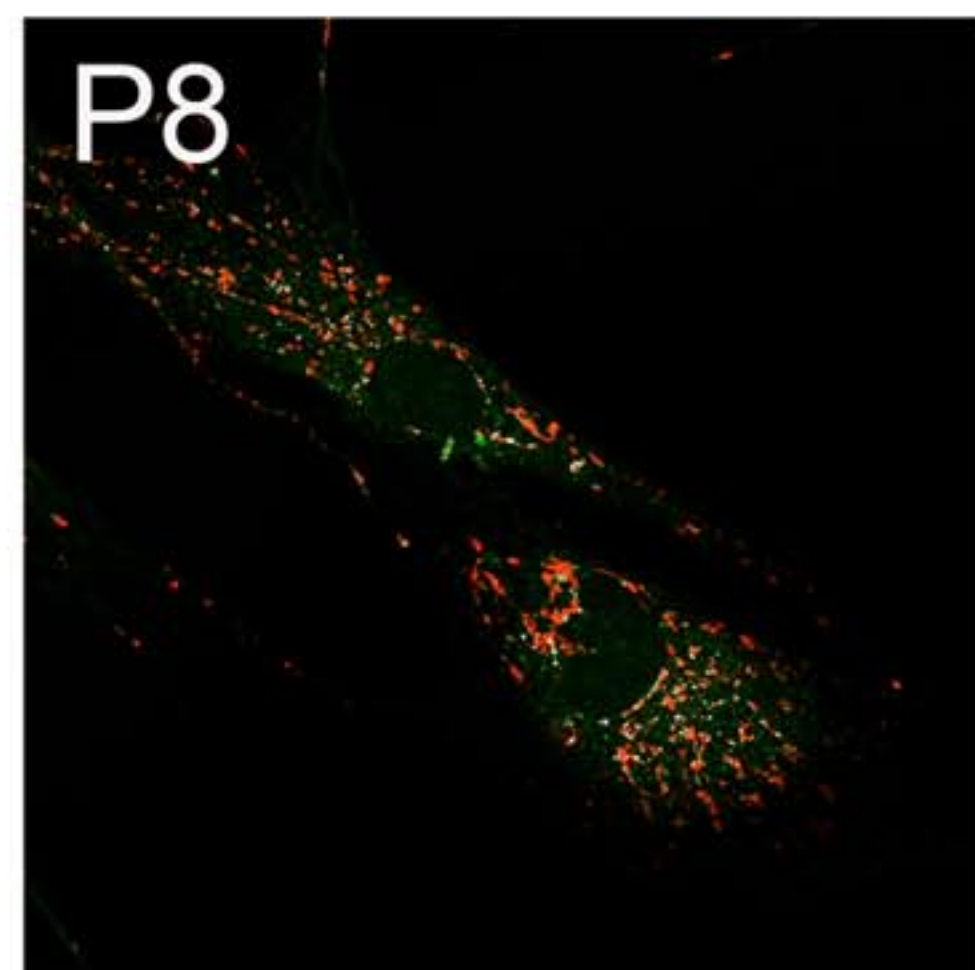
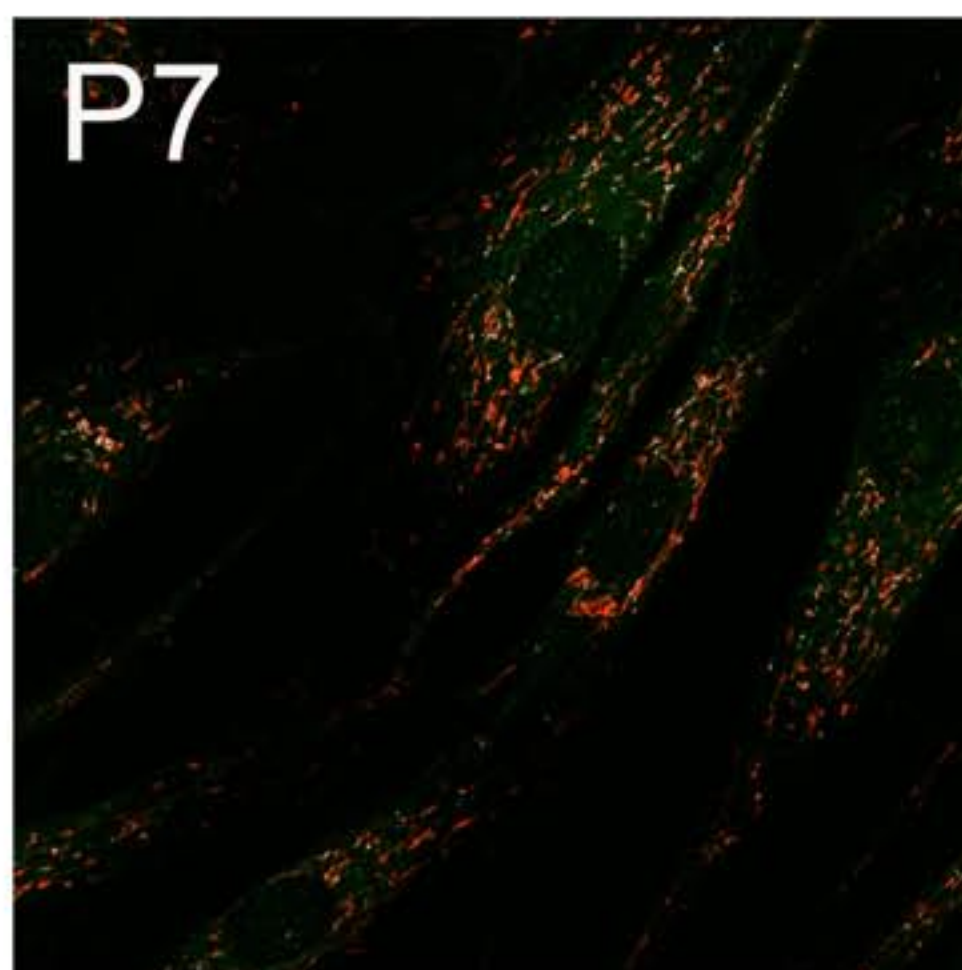
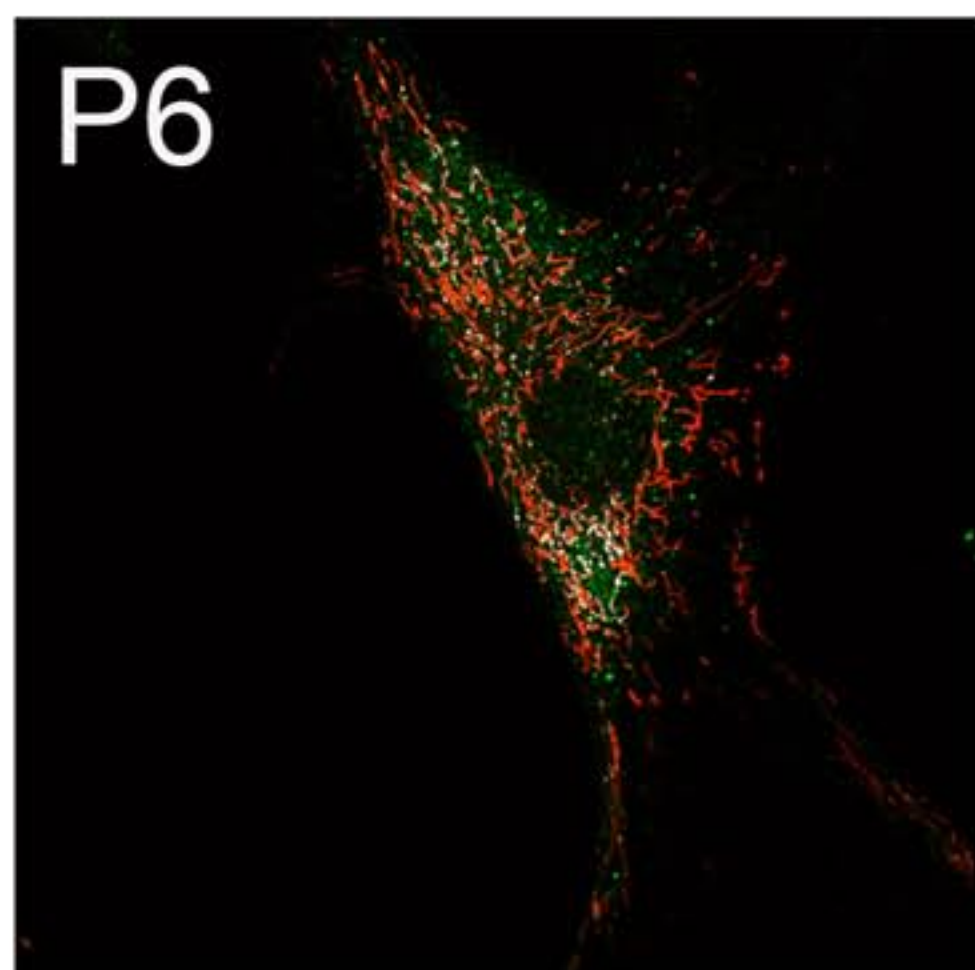
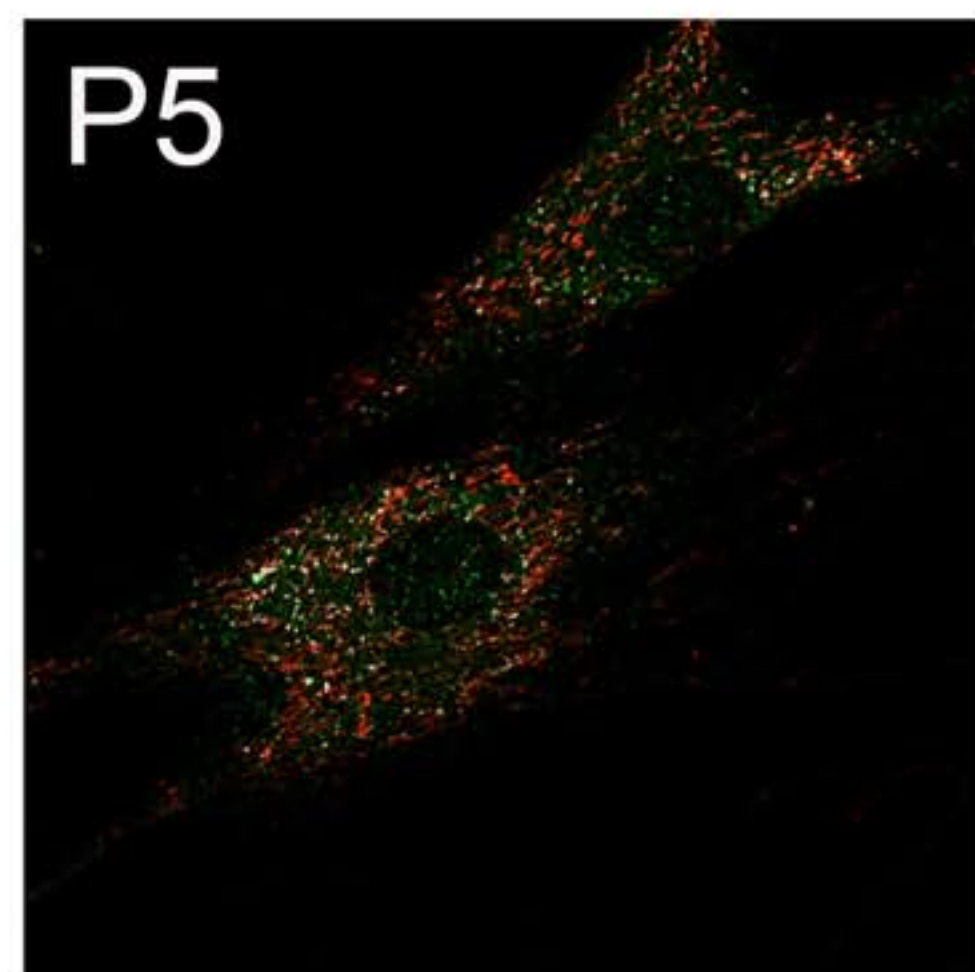
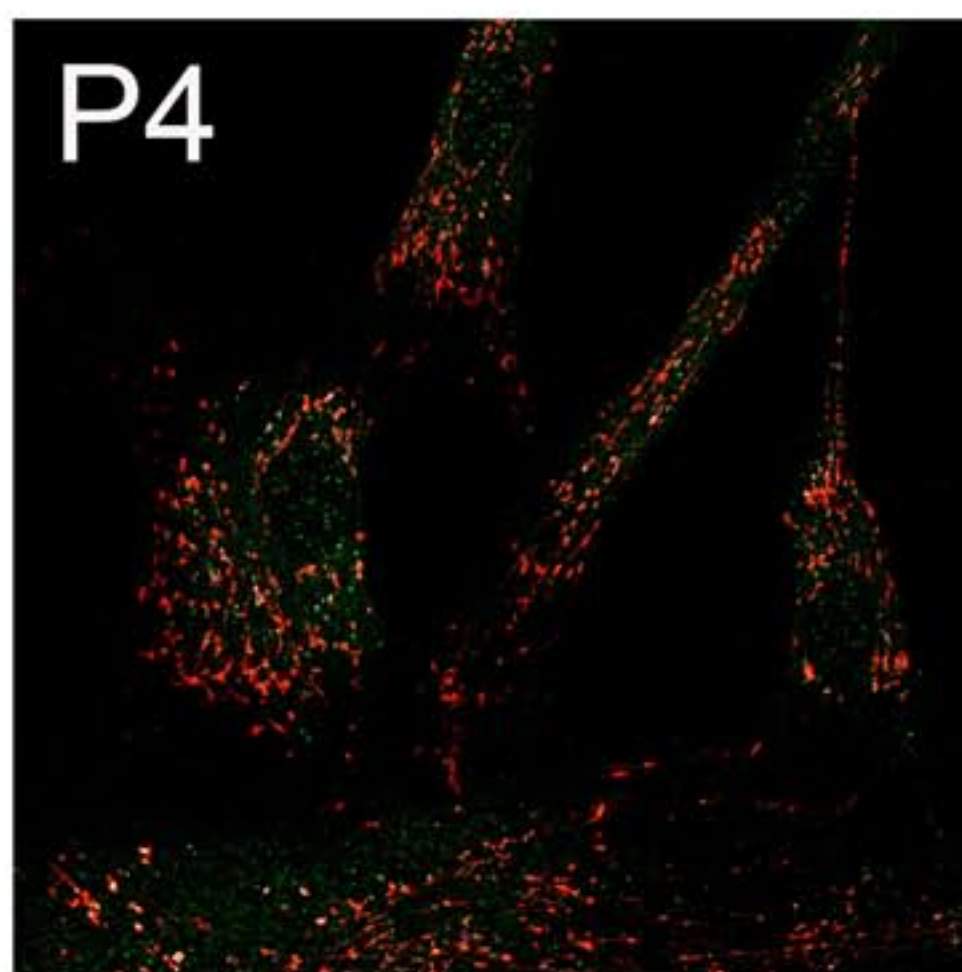
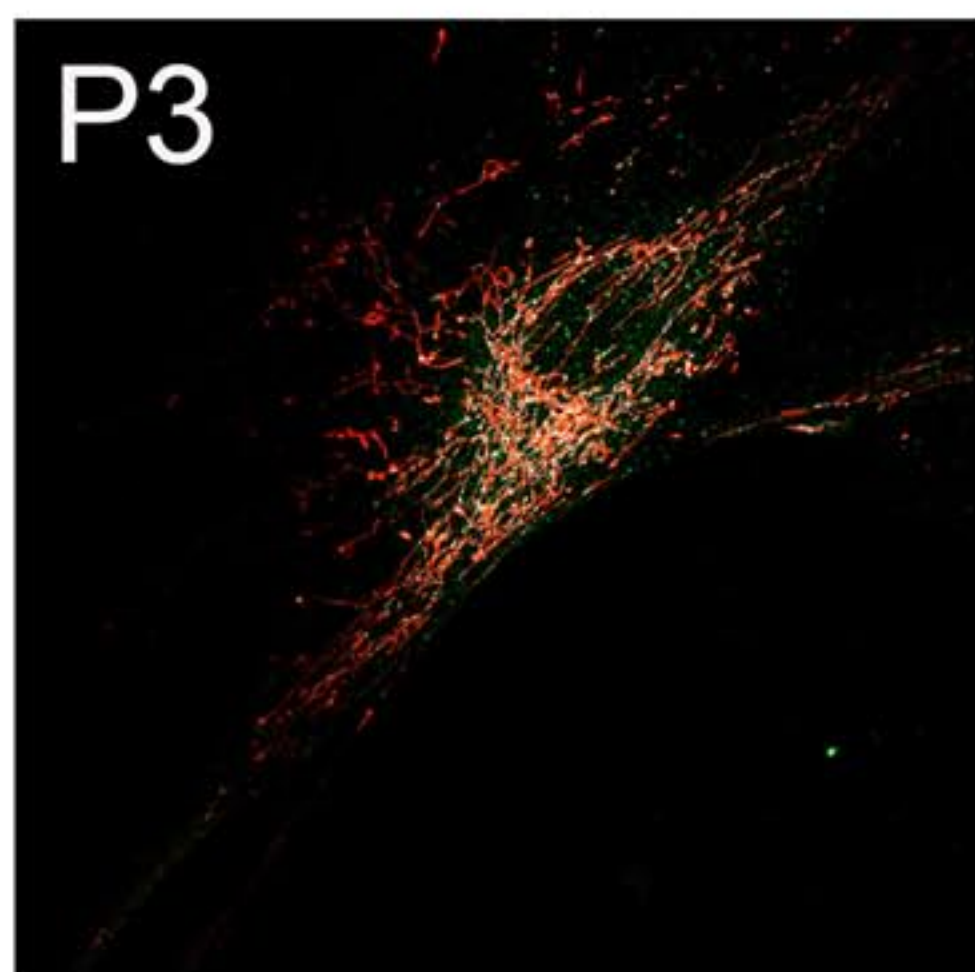
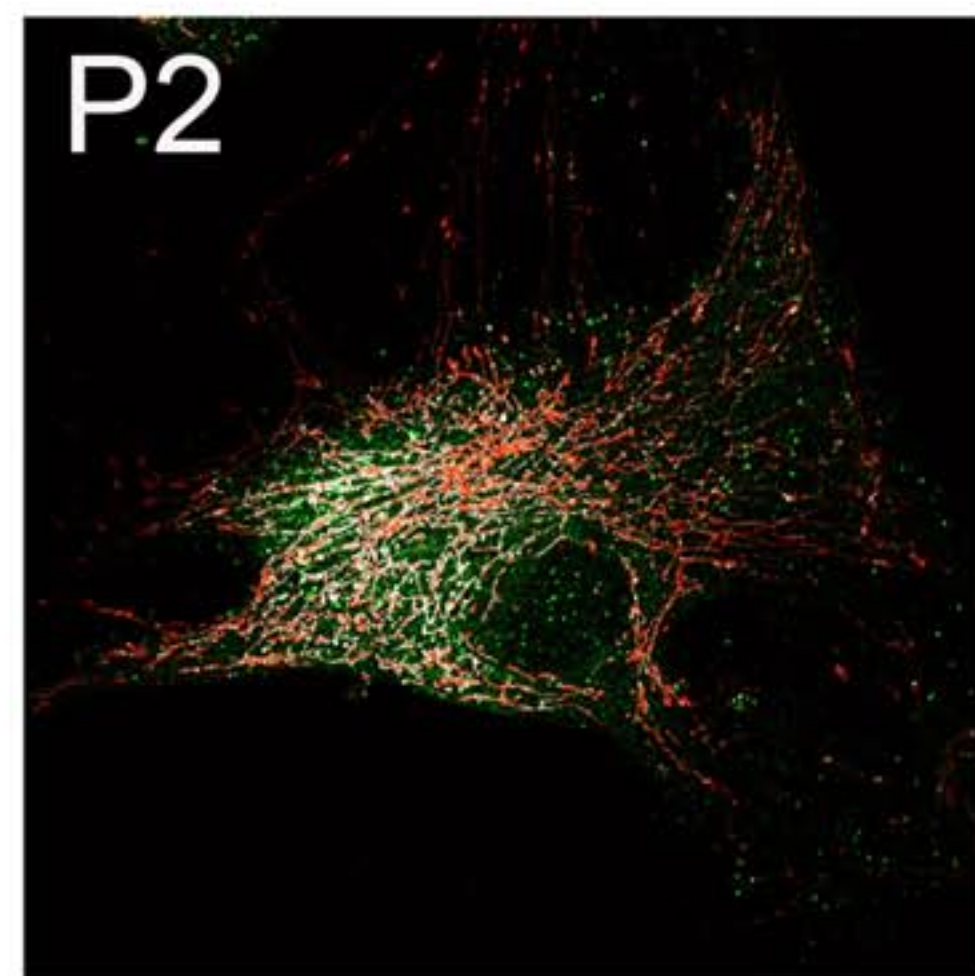
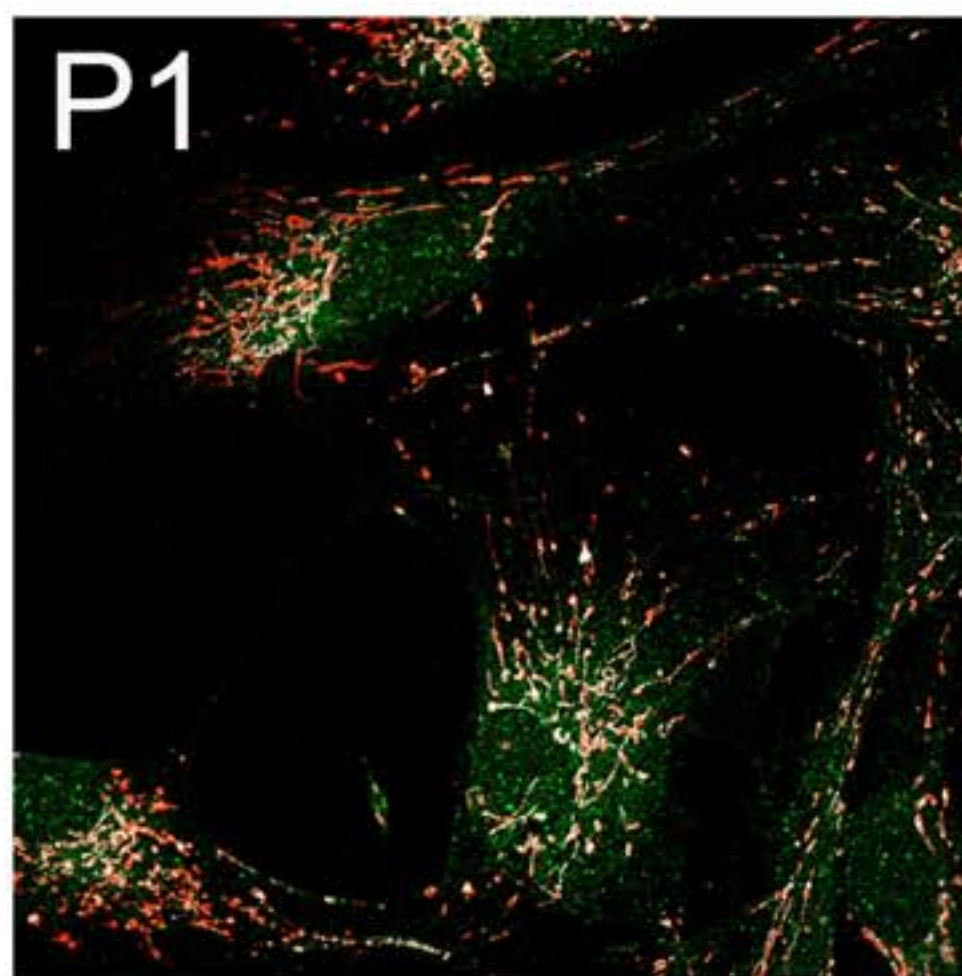
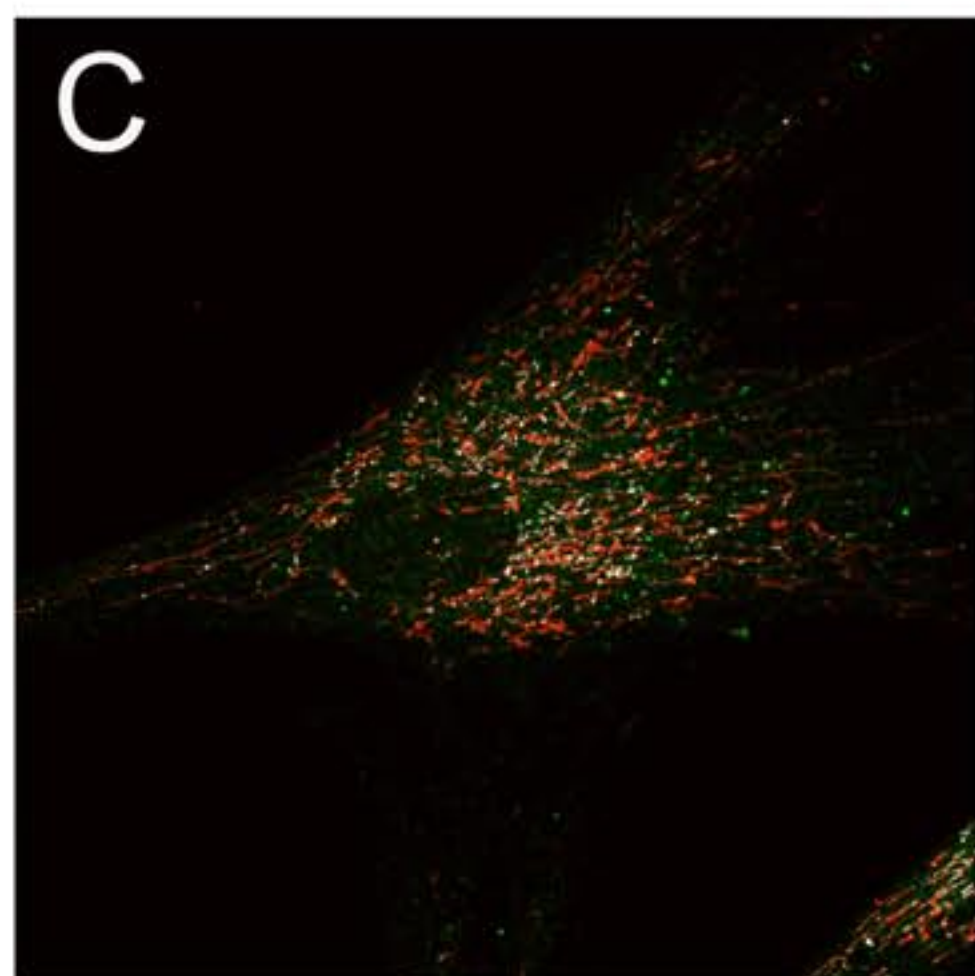
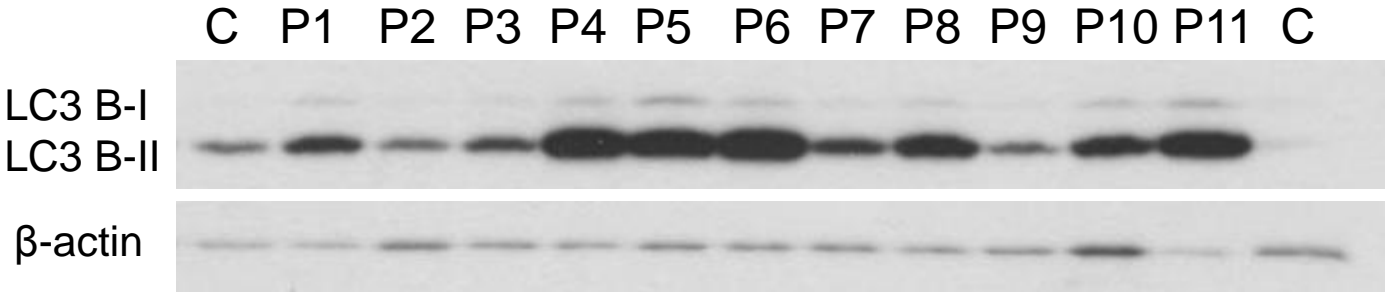
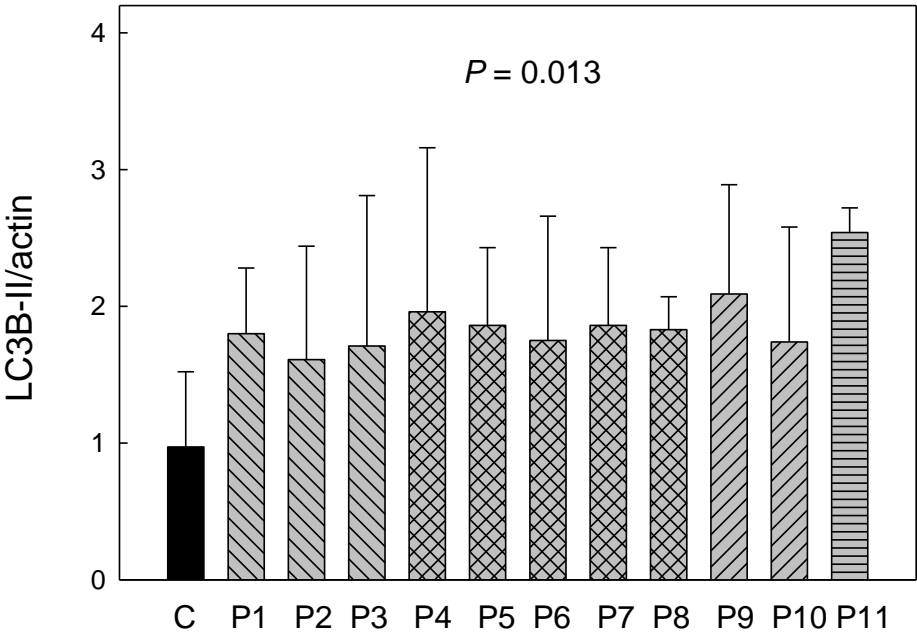


Figure 5

A



B



C

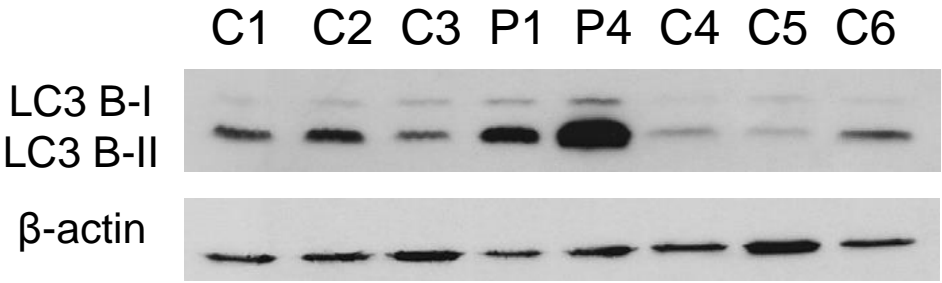
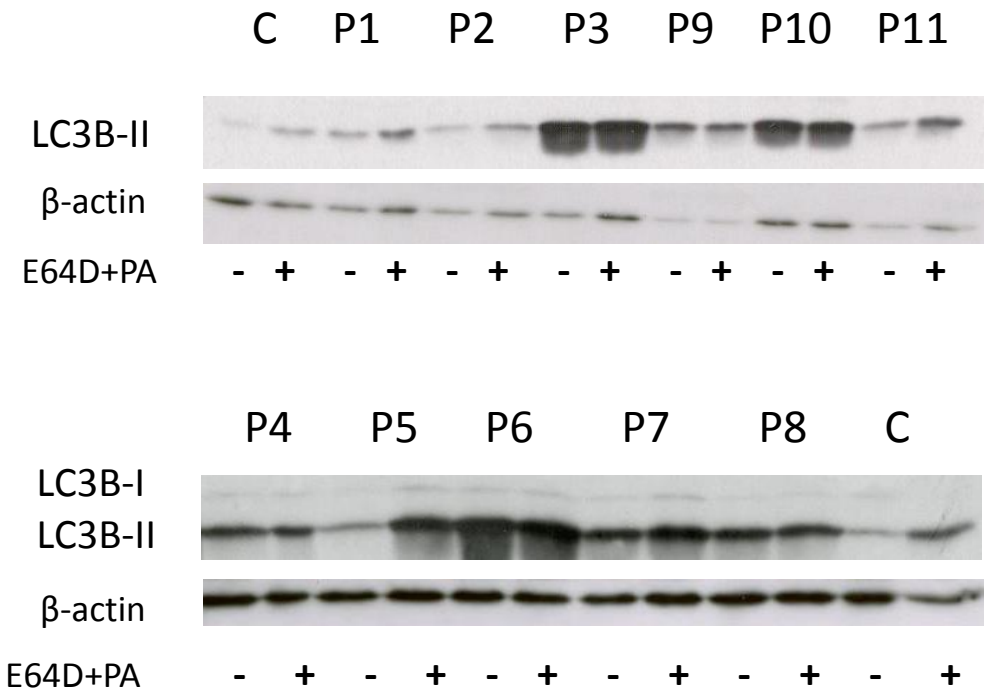


Figure 6

A



B

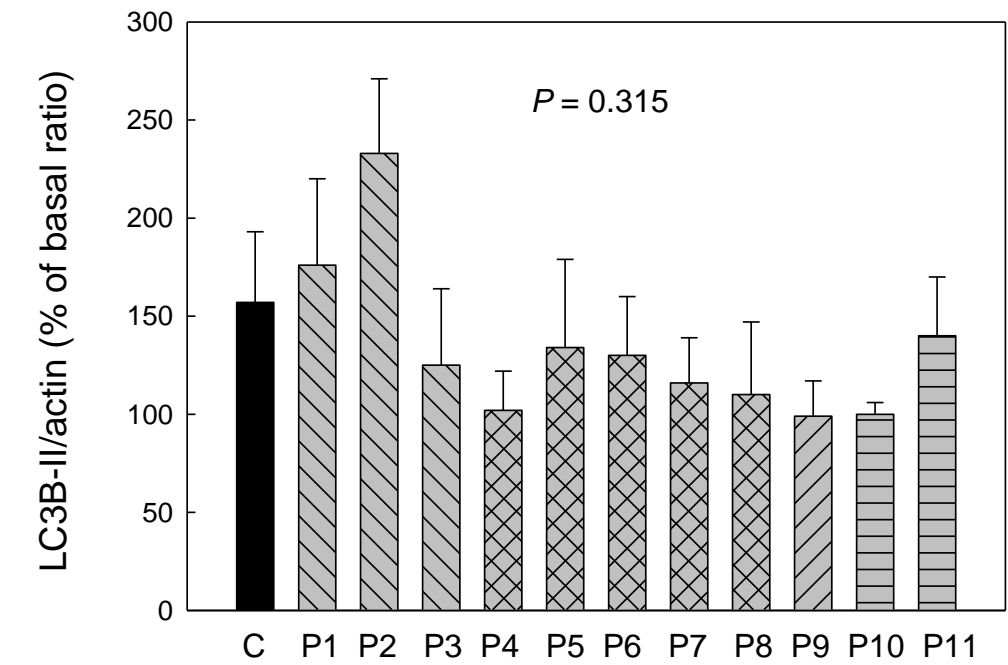


Figure 7

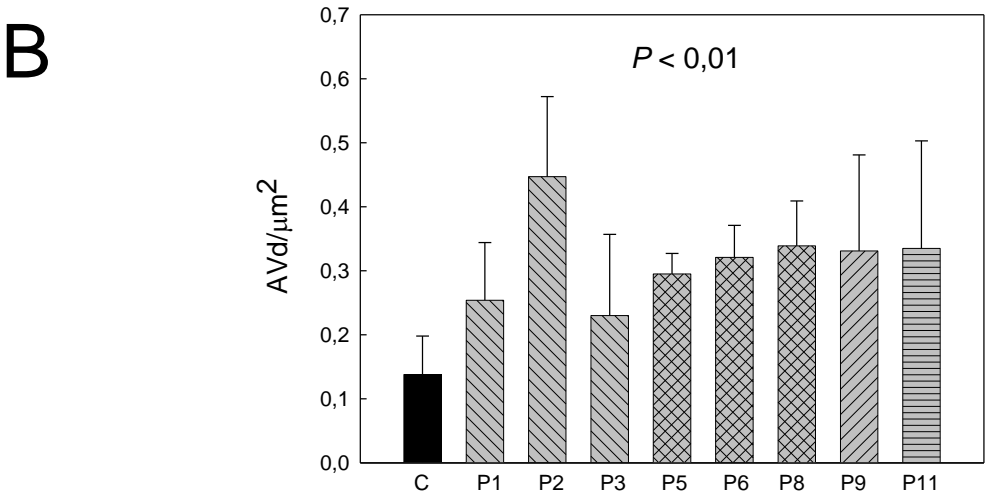
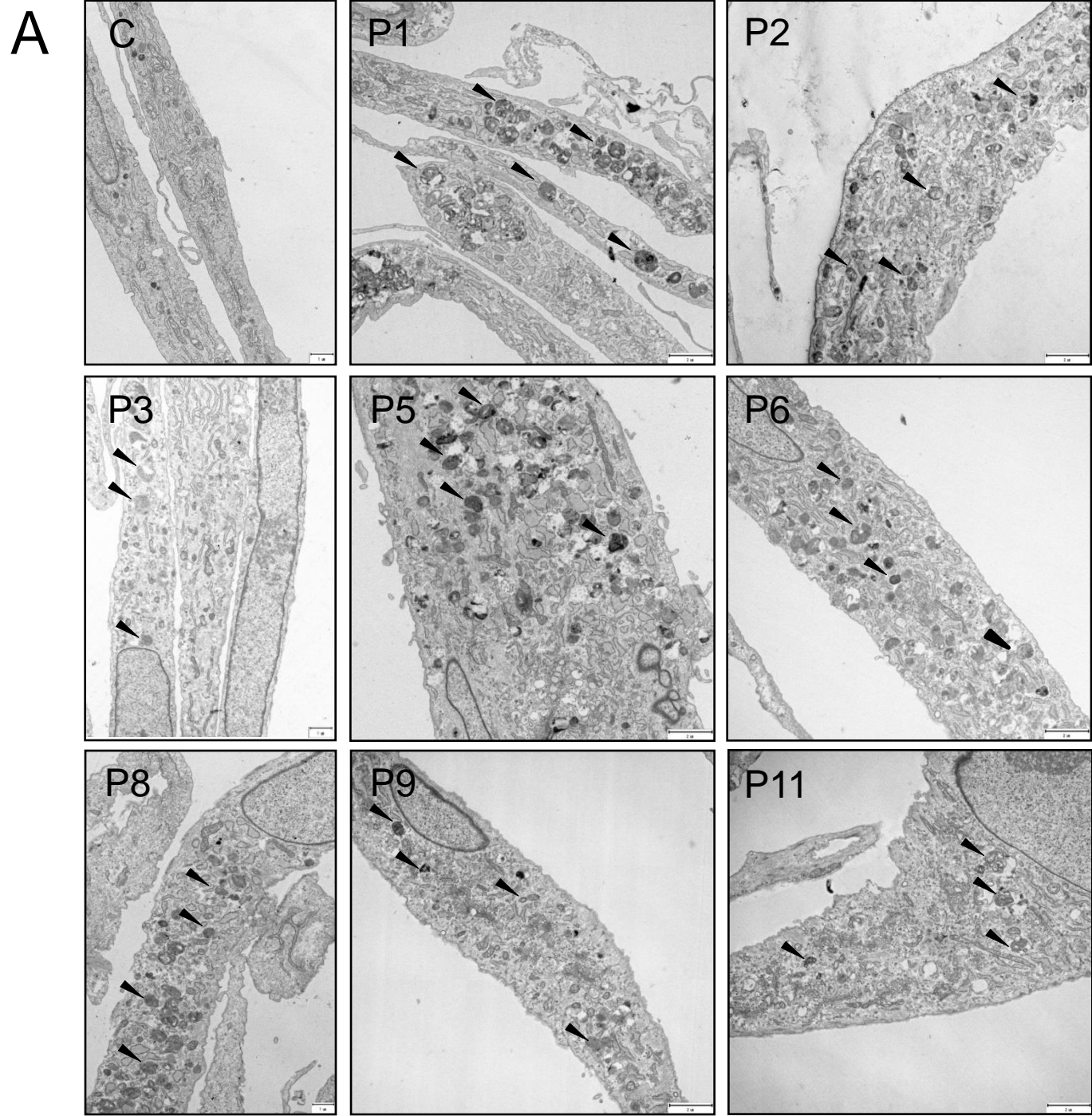
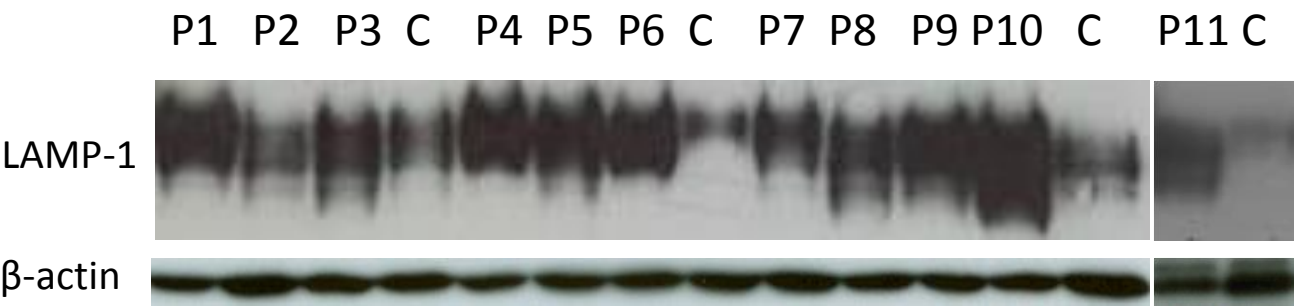
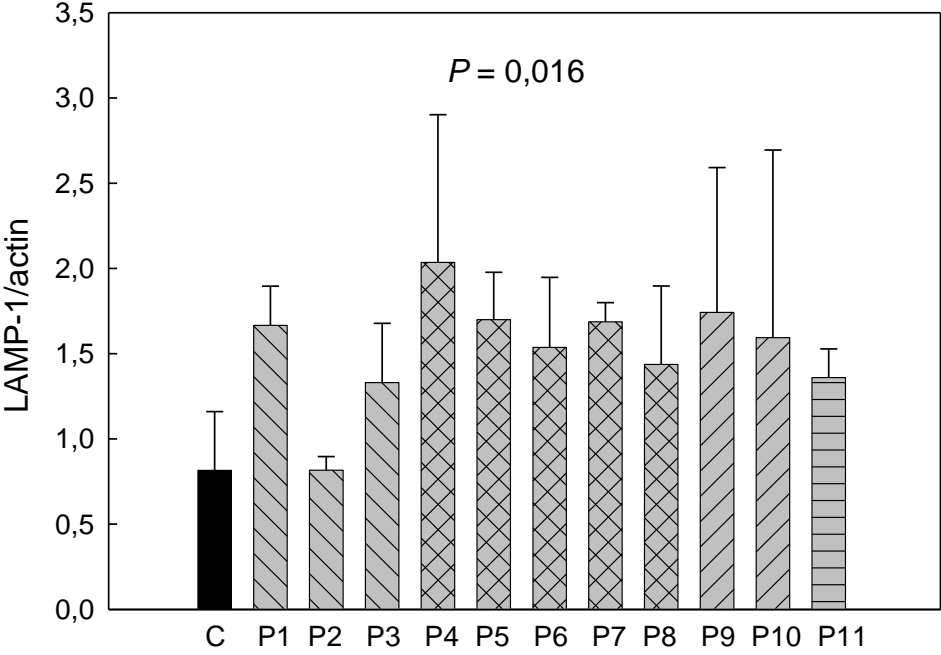


Figure 8

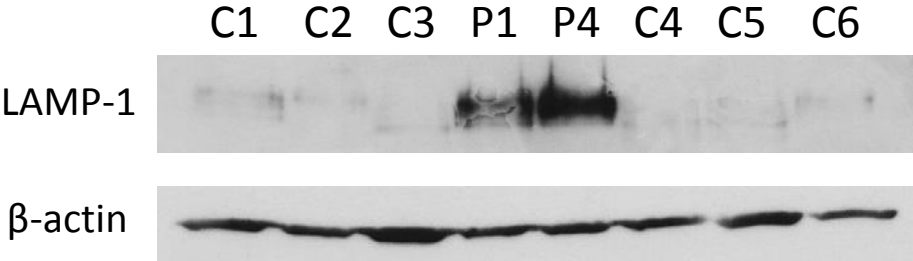
A



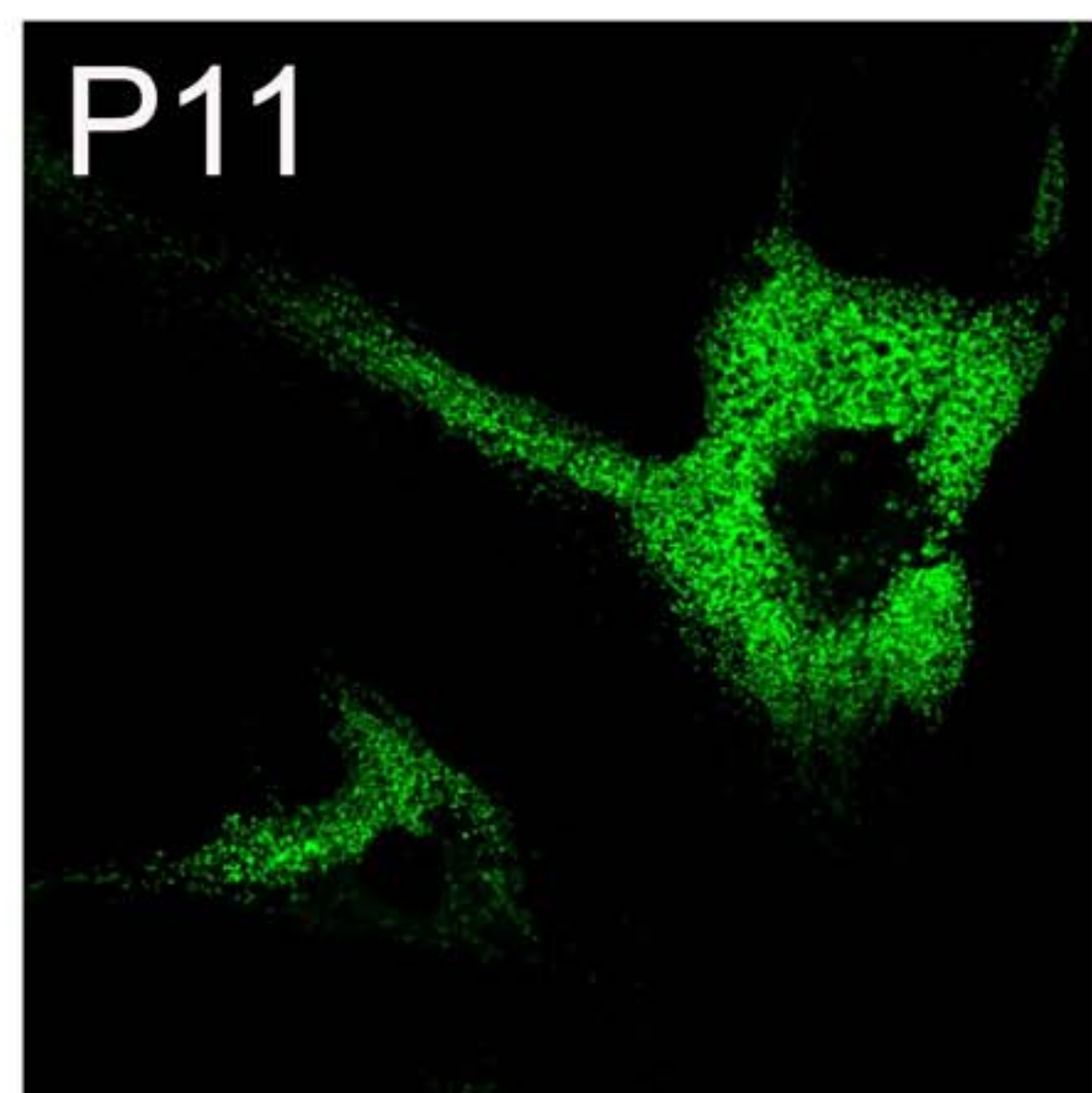
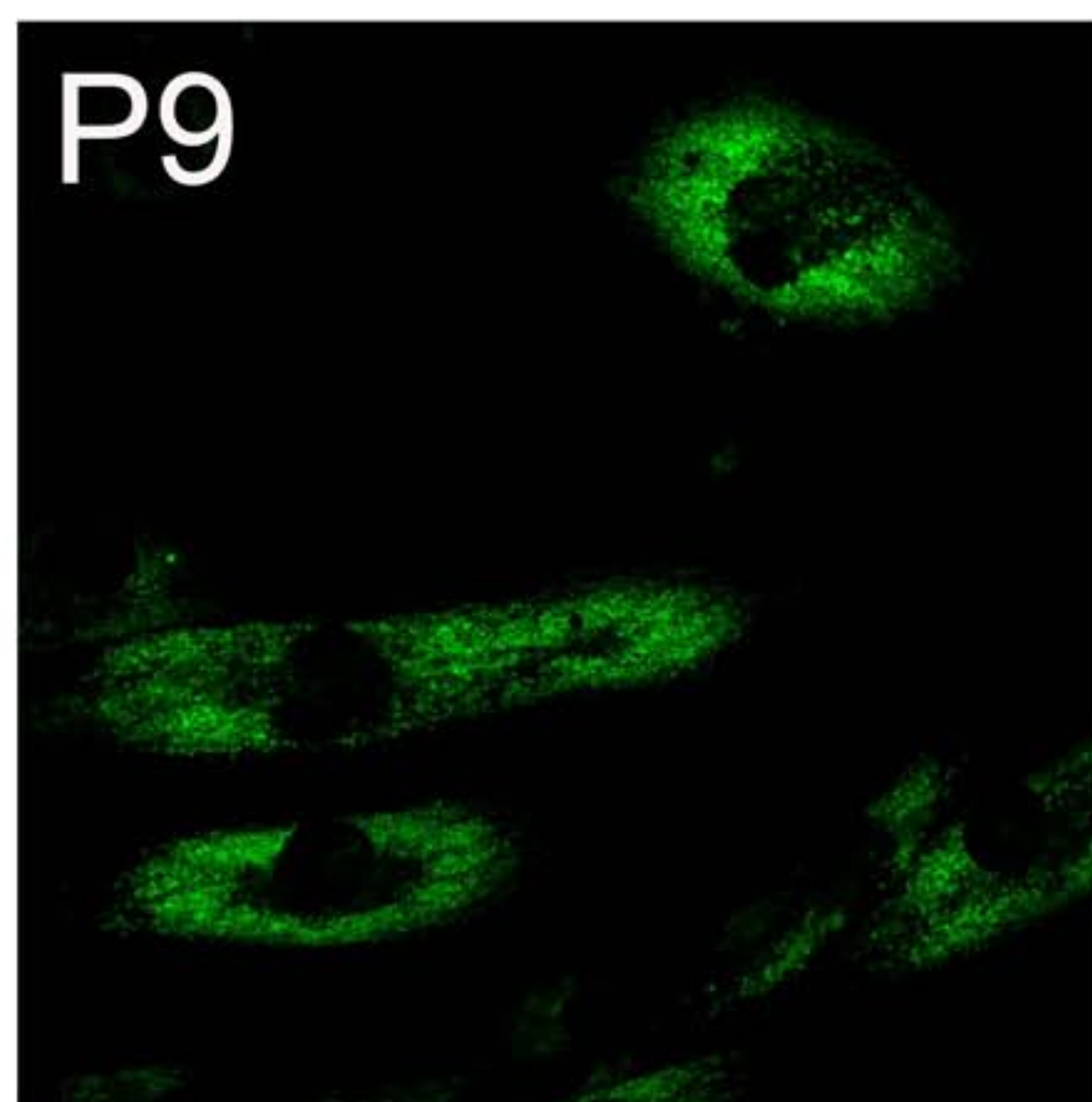
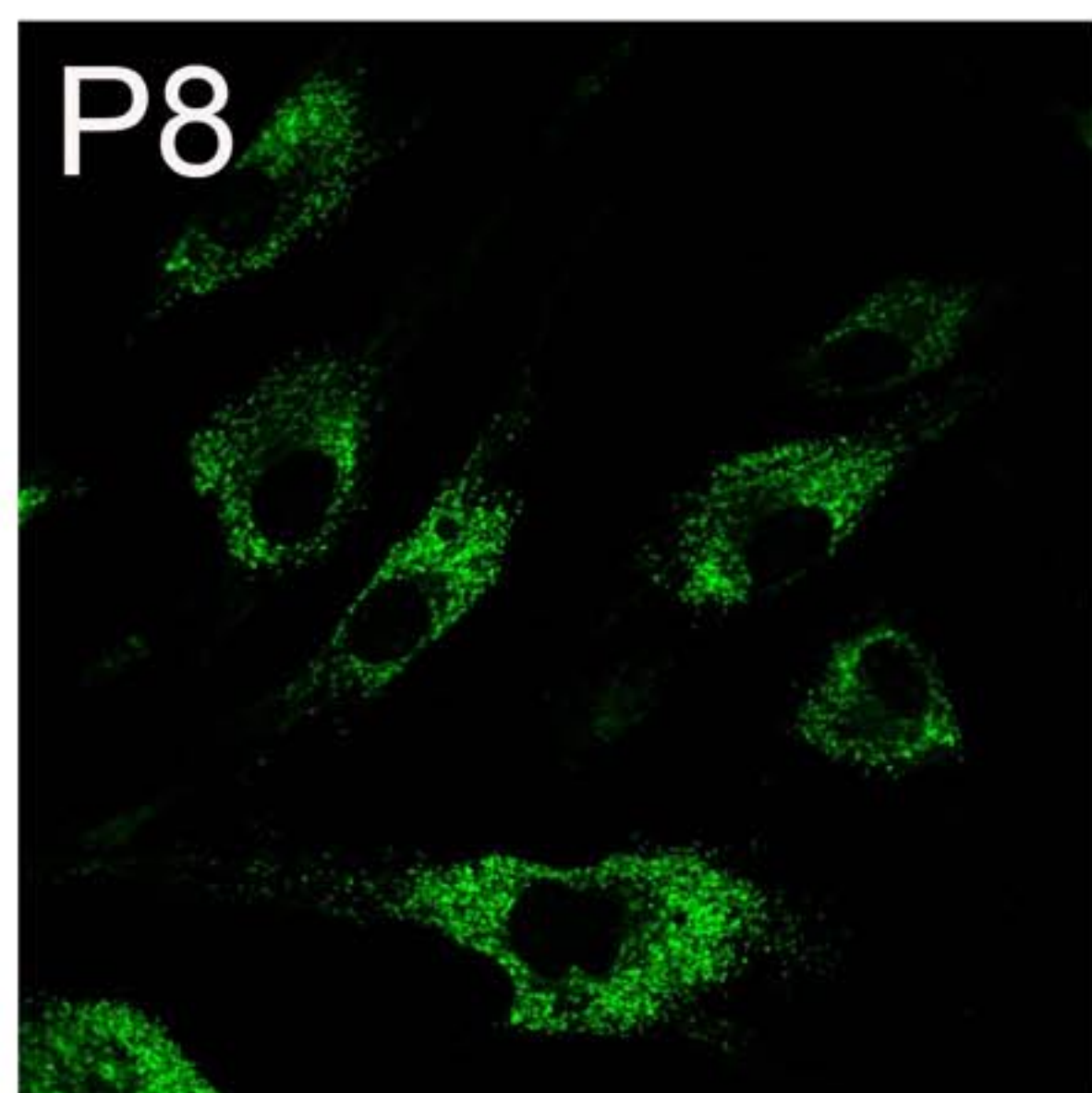
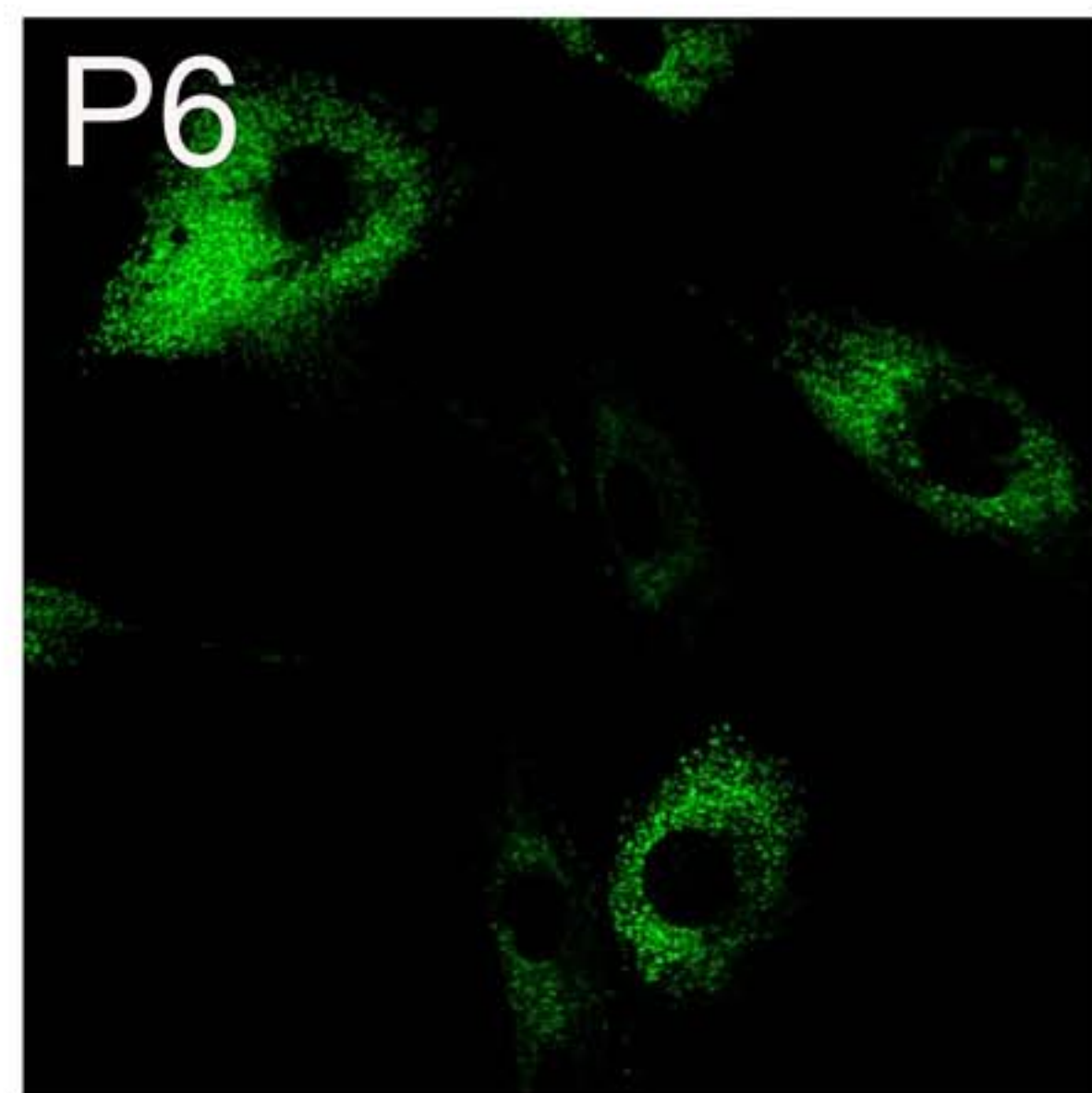
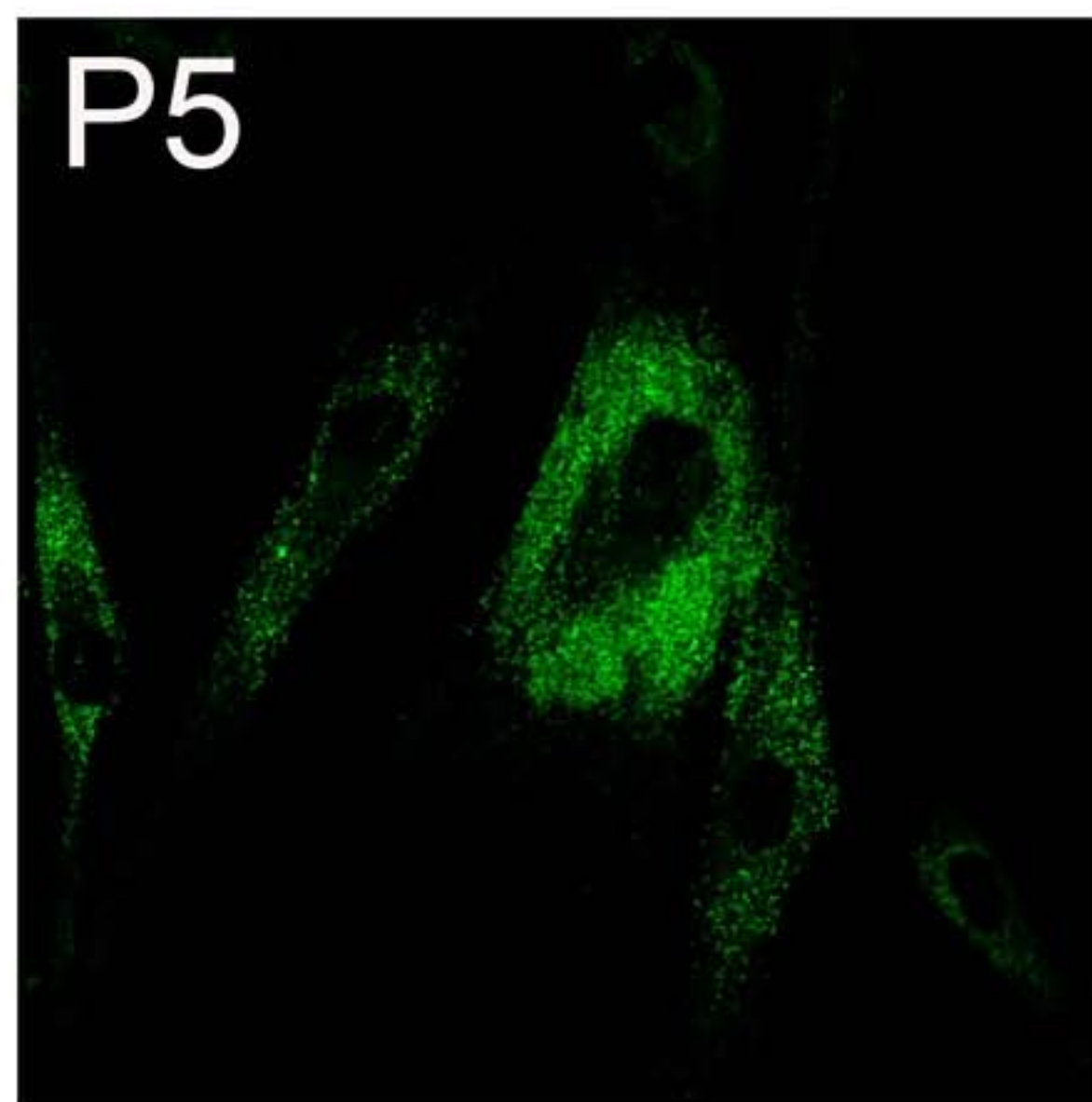
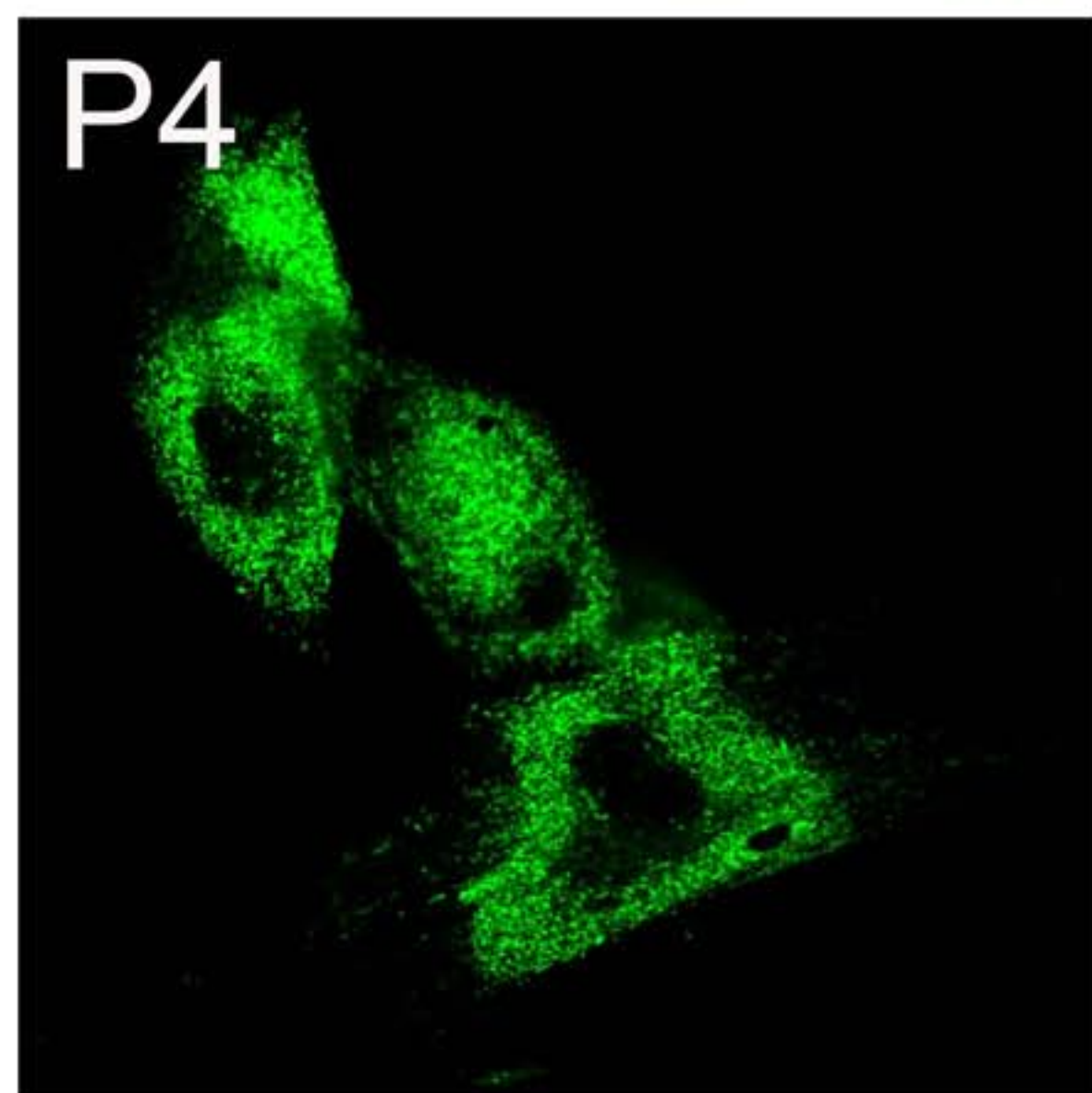
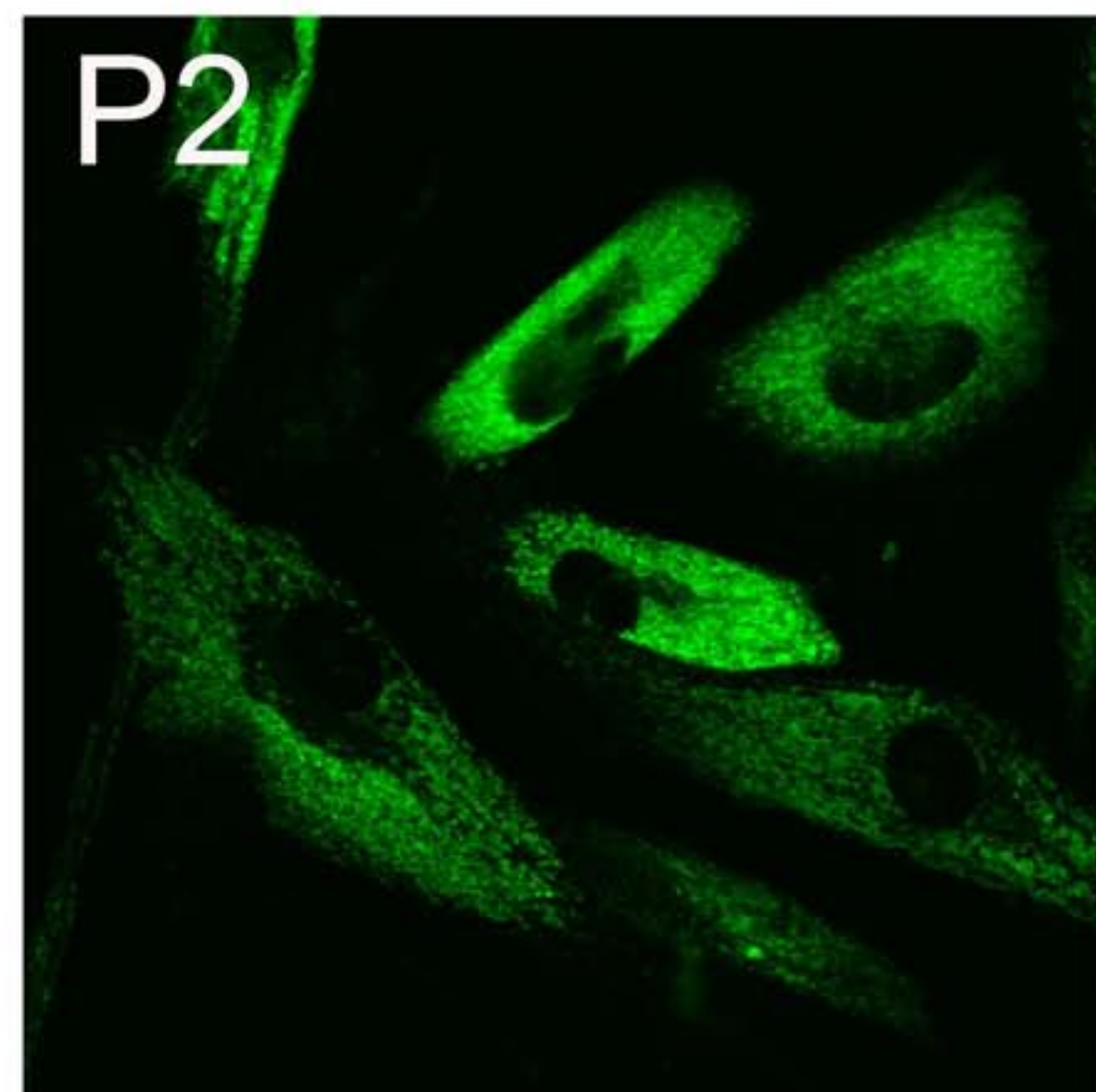
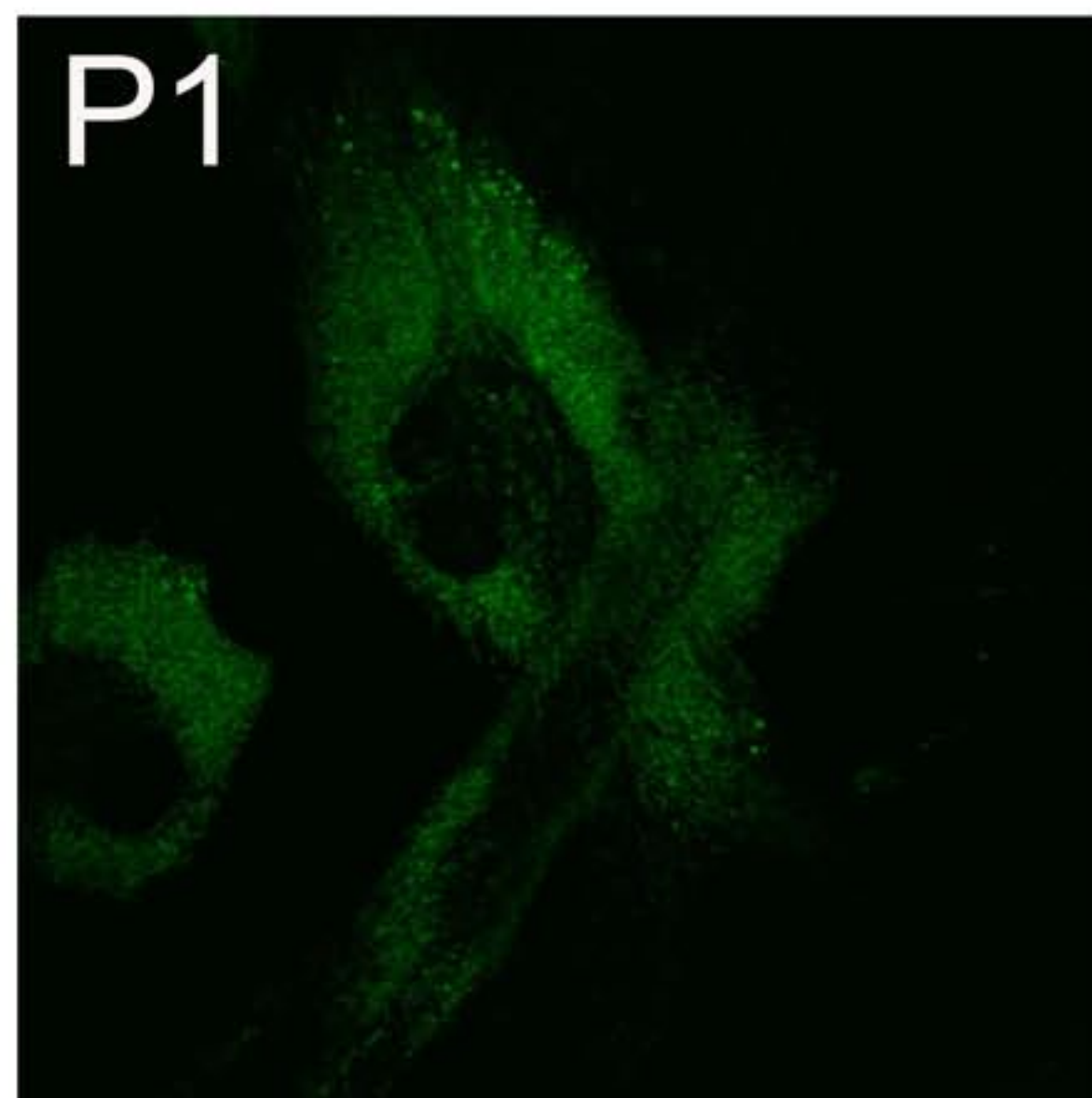
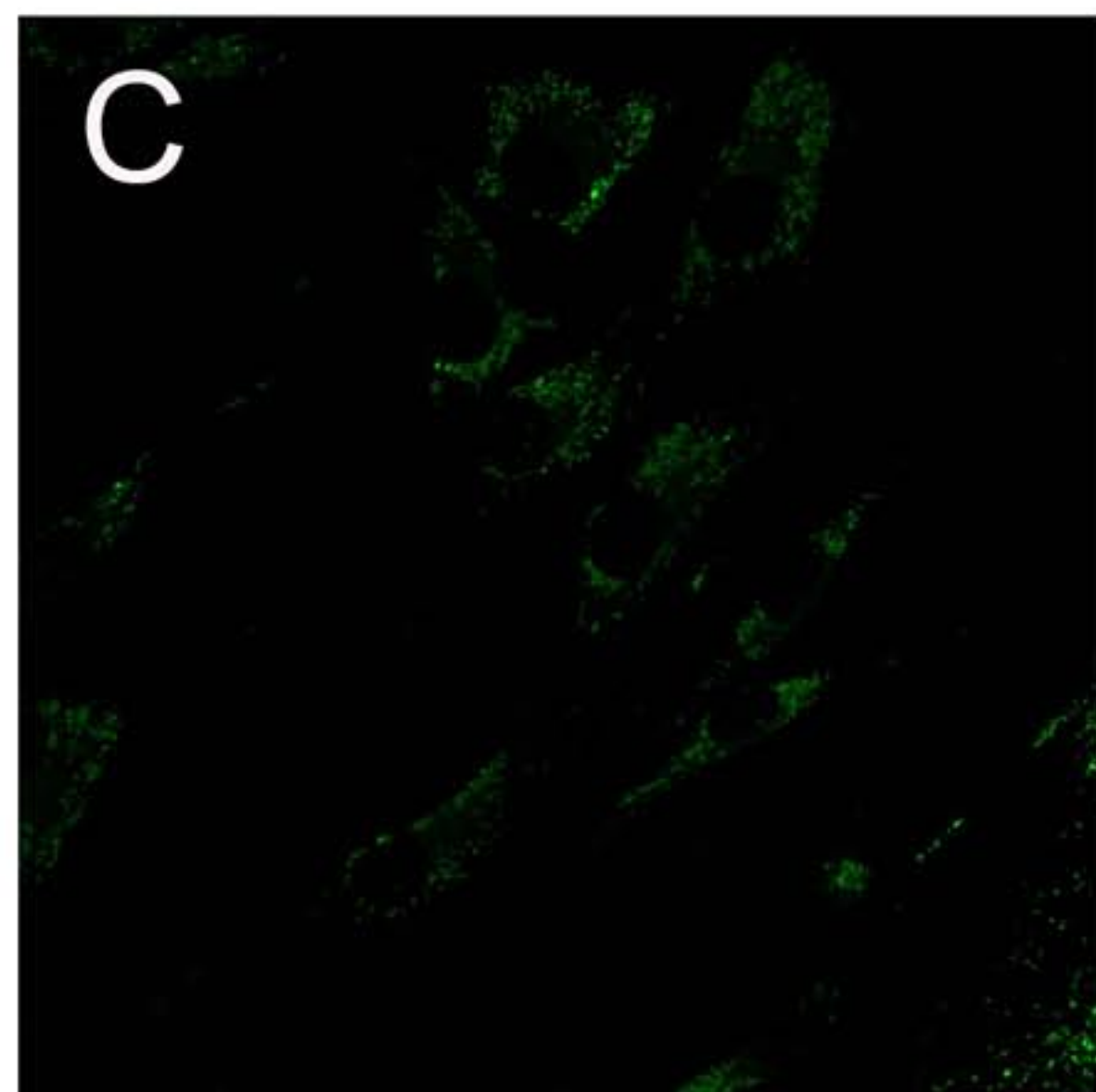
B



C



A



B

